Article:
Nguyen, V.T.T., Ulamec, S.M., Brockwell, D. et al. (Accepted: 2026) In silico peptide self-assembly reveals the importance of N-terminal motifs and the inhibition mechanism of the mutation L38M in α-synuclein fibrillation. Protein Science. ISSN: 0961-8368 (In Press)

Supplementary Material for the Publication
In silico peptide self-assembly reveals the importance of N-terminal motifs and the inhibition mechanism of L38M mutation in α-synuclein fibrillation

Van T. T. Nguyen[1] | Sabine M. Ulamec[2] | David J. Brockwell[2] | Sheena E. Radford[2] | Carol K. Hall[1]

[1]Department of Chemical and Biomolecular Engineering, North Carolina State University, Raleigh, North Carolina, USA

[2]Astbury Centre for Structural Molecular Biology, School of Molecular and Cellular Biology, Faculty of Biological Sciences, University of Leeds, Leeds LS2 9JT, UK.

*Corresponding Author

Email: hall@ncsu.edu

Supplementary Table

Table S1. Overview of the primary 59 computational simulations conducted.

Simulation ID	Number of chains	Concentration (mM)	Simulation Temperature		Duration		Results	Final snapshot
			Reduced unit	Kelvin	Billion collisions	μs		
P1-WT-Run1	48	10	0.186	310	300	32.0686	Aggregated with 6% antiparallel residues	Fig.S5
P1-WT-Run2	48	10	0.186	310	300	31.976	Aggregated with 8% antiparallel residues	Fig.S5
P1-WT-Run3	48	10	0.186	310	300	31.9204	Aggregated with 17% antiparallel residues	Fig.S5
P1-L38M-Run1	48	10	0.186	310	300	32.2089	Aggregated with 36% antiparallel residues	Fig.S5
P1-L38M-Run2	48	10	0.186	310	300	32.1964	Aggregated with 29% antiparallel residues	Fig.S5
P1-L38M-Run3	48	10	0.186	310	300	32.1929	Aggregated with 39% antiparallel residues	Fig.S5
P1-L38A-Run1	48	10	0.186	310	300	31.1666	Aggregated with 6% antiparallel residues	Fig.S5
P1-L38A-Run2	48	10	0.186	310	300	31.2339	Aggregated with 2% antiparallel residues	Fig.S5
P1-L38A-Run3	48	10	0.186	310	300	31.2336	Aggregated with 1% antiparallel residues	Fig.S5
P1-V40A-Run1	48	10	0.186	310	300	31.4239	Aggregated with 5% antiparallel residues	Fig.S5
P1-V40A-Run2	48	10	0.186	310	300	31.377	Aggregated with 19% antiparallel residues	Fig.S5
P1-V40A-Run3	48	10	0.186	310	300	31.4737	Aggregated with 6% antiparallel residues	Fig.S5

Table S2. Overview of the primary 59 computational simulations conducted (Continued).

Simulation ID	Number of chains	Concentration (mM)	Simulation Temperature		Duration		Results	Final snapshot
			Reduced unit	Kelvin	Billion collisions	μs		
P2-Run1	24	10	0.185	307	300	40.3907	Aggregated into a parallel U-shaped fibril	Fig.3a
P2-Run2	24	10	0.185	307	300	40.0085	Early stage of aggregation	none
P2-Run3	24	10	0.185	307	300	40.1762	Aggregated into a parallel S-shaped fibril	Fig.3a
P3-WT-Run1	24	10	0.195	330	500	38.8756	Aggregated into a mixed flat fibril	Fig.3b
P3-WT-Run2	24	10	0.195	330	500	38.9481	Aggregated into a mixed flat fibril	Fig.3b
P3-WT-Run3	24	10	0.195	330	500	38.8518	Aggregated into a mixed flat fibril	Fig3b
P3-WT-Run4	24	10	0.195	330	500	38.8504	Aggregated into a mixed flat fibril	Fig.3b
P3-L38M-Run1	24	10	0.195	330	500	38.7308	Aggregated into an antiparallel flat fibril	Fig.S7
P3-L38M-Run2	24	10	0.195	330	500	38.8477	Aggregated into a mixed flat fibril	Fig.S7
P3-L38M-Run3	24	10	0.195	330	500	38.9436	Aggregated into a mixed flat fibril	Fig.S7
P3-L38M-Run4	24	10	0.195	330	500	38.8338	Aggregated into an antiparallel flat fibril	Fig.S7
P3-L38A-Run1	24	10	0.195	330	500	38.6355	Aggregated into a mixed flat fibril	Fig.S7
P3-L38A-Run2	24	10	0.195	330	500	38.3531	Non-aggregated	Fig.S7
P3-L38A-Run3	24	10	0.195	330	500	38.3533	Non-aggregated	Fig.S7
P3-L38A-Run4	24	10	0.195	330	500	38.3515	Non-aggregated	Fig.S7

Table S3. Overview of the primary 59 computational simulations conducted (Continued).

Simulation ID	Number of chains	Concentration (mM)	Simulation Temperature		Duration		Results	Final snapshot
			Reduced unit	Kelvin	Billion collisions	μs		
P3-V40A-Run1	24	10	0.195	330	500	38.7247	Aggregated into a mixed flat fibril	Fig.S7
P3-V40A-Run2	24	10	0.195	330	500	38.4748	Non-aggregated	Fig.S7
P3-V40A-Run3	24	10	0.195	330	500	38.7651	Aggregated into a mixed flat fibril	Fig.S7
P3-V40A-Run4	24	10	0.195	330	500	38.4747	Non-aggregated	Fig.S7
P3Next-WT-Run1	24	10	0.195	330	700	38.1718	Aggregated with 21% β-hairpins	Fig.S4
P3Next-WT-Run2	24	10	0.195	330	700	38.1604	Aggregated with 21% β-hairpins	FigS4
P3Next-WT-Run3	24	10	0.195	330	700	38.2052	Aggregated with 22% β-hairpins	Fig.S4
P3Next-WT-Run4	24	10	0.195	330	700	38.1693	Aggregated with 29% β-hairpins	Fig.S4
P3Next-WT-Run5	24	10	0.195	330	700	38.2871	Aggregated with 21% β-hairpins	Fig.S4
P3Next-WT-Run6	24	10	0.195	330	700	38.2033	Aggregated with 25% β-hairpins	Fig.S4
P3Next-WT-Run7	24	10	0.195	330	700	38.1875	Aggregated with 21% β-hairpins	Fig.S4
P3Next-L38M-Run1	24	10	0.195	330	700	38.1701	Aggregated with 9% β-hairpins	Fig.S8
P3Next-L38M-Run2	24	10	0.195	330	700	38.344	Aggregated with 21% β-hairpins	Fig.S8
P3Next-L38M-Run3	24	10	0.195	330	700	38.3126	Aggregated with 13% β-hairpins	Fig.S8

Table S4. Overview of the primary 59 computational simulations conducted (Continued).

Simulation ID	Number of chains	Concentration (mM)	Simulation Temperature		Duration		Results	Final snapshot
			Reduced unit	Kelvin	Billion collisions	μs		
P3Next-L38M-Run4	24	10	0.195	330	500	38.1637	Aggregated with 22% β-hairpins	Fig.S8
P3Next-L38M-Run5	24	10	0.195	330	500	38.3195	Aggregated with 17% β-hairpins	Fig.S8
P3Next-L38M-Run6	24	10	0.195	330	500	38.3287	Aggregated with 17% β-hairpins	Fig.S8
P3Next-L38M-Run7	24	10	0.195	330	500	38.2088	Aggregated with 13% β-hairpins	Fig.S8
P3Next-L38A-Run1	24	10	0.195	330	700	37.8362	Aggregated with 60% β-hairpins	Fig.S9
P3Next-L38A-Run2	24	10	0.195	330	700	37.8362	Aggregated with 33% β-hairpins	FigS9
P3Next-L38A-Run3	24	10	0.195	330	700	37.7245	Non-aggregated	Fig.S9
P3Next-L38A-Run4	24	10	0.195	330	700	37.7505	Aggregated with 47% β-hairpins	Fig.S9
P3Next-L38A-Run5	24	10	0.195	330	700	37.7252	Non-aggregated	Fig.S9
P3Next-L38A-Run6	24	10	0.195	330	700	37.727	Aggregated with 67% β-hairpins	Fig.S9
P3Next-L38A-Run7	24	10	0.195	330	700	37.7493	Aggregated with 21% β-hairpins	Fig.S9
P3Next-V40A-Run1	24	10	0.195	330	700	37.8267	Aggregated with 41% β-hairpins	Fig.S10
P3Next-V40A-Run2	24	10	0.195	330	700	37.813	Non-aggregated	Fig.S10
P3Next-V40A-Run3	24	10	0.195	330	700	37.8962	Aggregated with 64% β-hairpins	Fig.S10

Table S5. Overview of the primary 59 computational simulations conducted (Continued).

Simulation ID	Number of chains	Concentration (mM)	Simulation Temperature		Duration		Results	Final snapshot
			Reduced unit	Kelvin	Billion collisions	μs		
P3Next-V40A-Run4	24	10	0.195	330	500	37.8165	Aggregated with 44% β-hairpins	Fig.S10
P3Next-V40A-Run5	24	10	0.195	330	500	38.0164	Aggregated with 24% β-hairpins	Fig.S10
P3Next-V40A-Run6	24	10	0.195	330	500	37.8496	Aggregated with 27% β-hairpins	Fig.S10
P3Next-V40A-Run7	24	10	0.195	330	500	38.0625	Aggregated with 18% β-hairpins	Fig.S10

Table S2. Overview of the additional 20 computational simulations conducted for Y39A and S42A.

Simulation ID	Number of chains	Concentration (mM)	Simulation Temperature		Duration		Results	Final snapshot
			Reduced unit	Kelvin	Billion collisions	μs		
P1-Y39A-Run1	48	10	0.186	310	300	30.9294	Aggregated with 26% antiparallel residues	Fig.S18
P1-Y39A-Run2	48	10	0.186	310	300	30.9262	Aggregated with 33% antiparallel residues	Fig.S18
P1-Y39A-Run3	48	10	0.186	310	300	30.9410	Aggregated with 31% antiparallel residues	Fig.S18
P1-S42A-Run1	48	10	0.186	310	300	31.5424	Aggregated with 12% antiparallel residues	Fig.S18
P1-S42A-Run2	48	10	0.186	310	300	31.5569	Aggregated with 15% antiparallel residues	Fig.S18
P1-S42A-Run3	48	10	0.186	310	300	31.5605	Aggregated with 15% antiparallel residues	Fig.S18
P3Next-Y39A-Run1	24	10	0.195	330	700	37.8839	Aggregated with 39% β-hairpins	Fig.S20
P3Next-Y39A-Run2	24	10	0.195	330	700	37.8501	Aggregated with 29% β-hairpins	FigS20
P3Next-Y39A-Run3	24	10	0.195	330	700	37.9191	Aggregated with 32% β-hairpins	Fig.S20
P3Next-Y39A-Run4	24	10	0.195	330	700	37.9006	Aggregated with 35% β-hairpins	Fig.S20
P3Next-Y39A-Run5	24	10	0.195	330	700	37.9183	Aggregated with 41% β-hairpins	Fig.S20
P3Next-Y39A-Run6	24	10	0.195	330	700	37.9674	Aggregated with 17% β-hairpins	Fig.S20
P3Next-Y39A-Run7	24	10	0.195	330	700	38.0385	Aggregated with 21% β-hairpins	Fig.S20

Table S2. Overview of the additional 20 computational simulations conducted for Y39A and S42A (Continued).

Simulation ID	Number of chains	Concentration (mM)	Simulation Temperature		Duration		Results	Final snapshot
			Reduced unit	Kelvin	Billion collisions	μs		
P3Next-S42A-Run1	24	10	0.195	330	700	37.9986	Aggregated with 32% β-hairpins	Fig.S21
P3Next-S42A-Run2	24	10	0.195	330	700	38.1418	Aggregated with 14% β-hairpins	FigS21
P3Next-S42A-Run3	24	10	0.195	330	700	38.0774	Aggregated with 18% β-hairpins	Fig.S21
P3Next-S42A-Run4	24	10	0.195	330	700	38.0321	Aggregated with 21% β-hairpins	Fig.S21
P3Next-S42A-Run5	24	10	0.195	330	700	38.0709	Aggregated with 38% β-hairpins	Fig.S21
P3Next-S42A-Run6	24	10	0.195	330	700	38.1372	Aggregated with 17% β-hairpins	Fig.S21
P3Next-S42A-Run7	24	10	0.195	330	700	37.8714	Aggregated with 25% β-hairpins	Fig.S21

Supplementary Figures

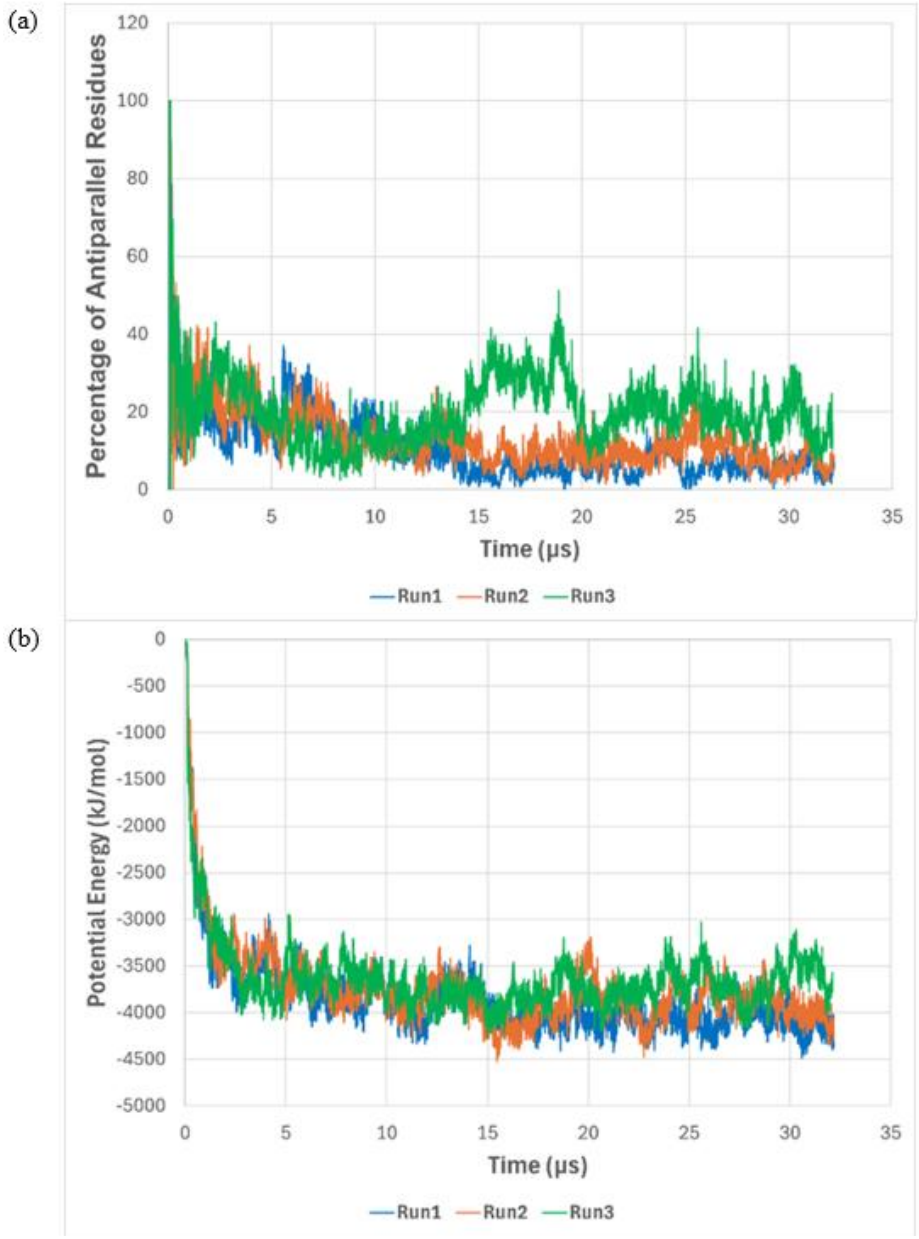

Figure S1 Time evolution of (a) percentage of antiparallel residues and (b) potential energy in P1-WT simulations

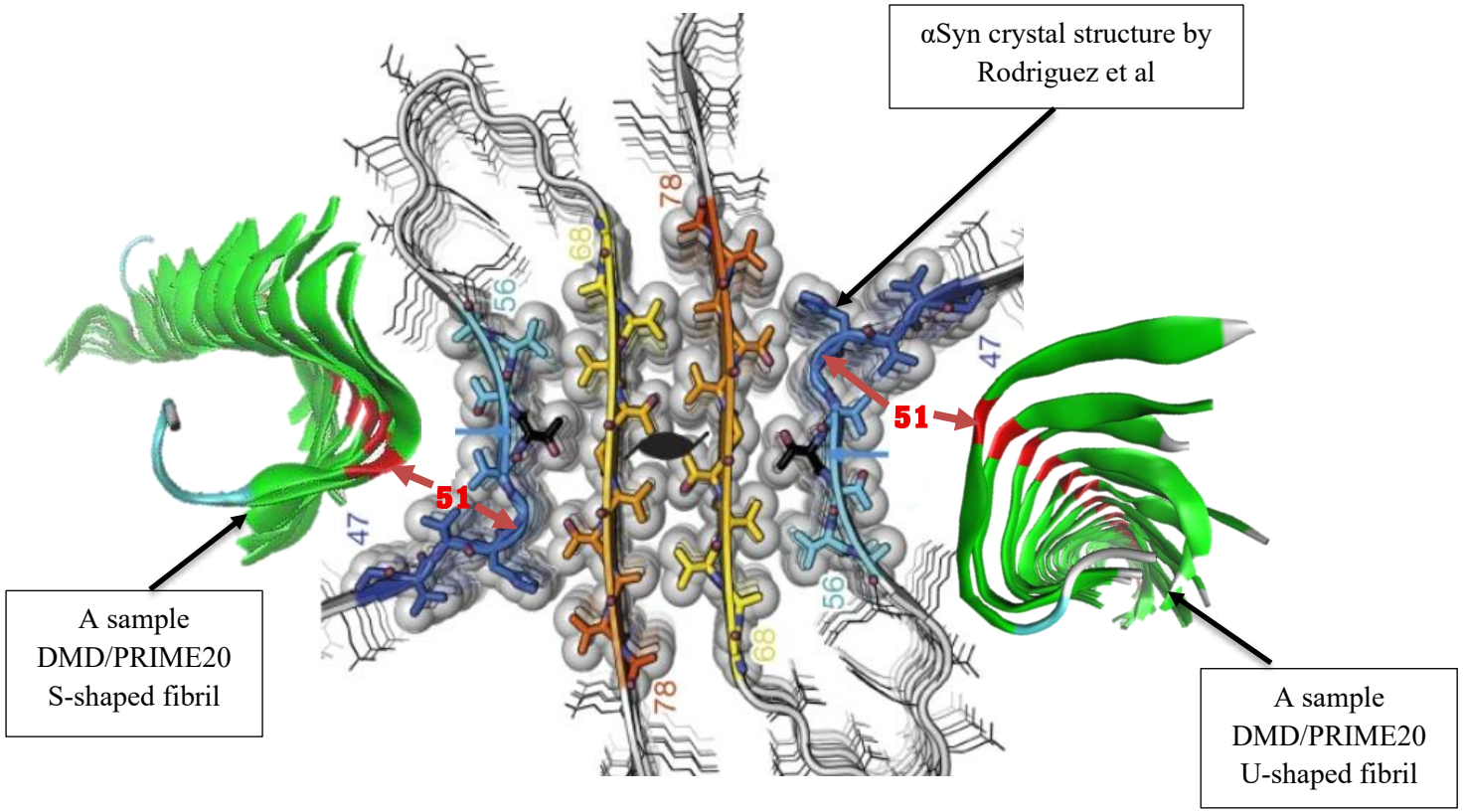

Figure S2. DMD/PRIME20 simulated structures of the P2 peptide (αSyn[45–57]) are presented alongside the PreNAC region (αSyn[47–56]) of the nanocrystal structure to highlight similarities in key structural features. The center structure is the atomistic model of the αSyn nanocrystal structure of αSyn[47–56] reported by Rodriguez et al. (Rodriguez et al. 2015). The structure shows the PreNAC fragment in blue and the NAC core in orange. The PreNAC fragments form in-register parallel β-strands with a characteristic bend at Gly51. In comparison, the green structures positioned to the left and right of the crystal structure correspond to the S-shaped and U-shaped fibrillar conformations formed by P2 peptides in our DMD/PRIME20 simulations. Our simulations predicted single-layer parallel β-sheets that curve around Gly51 (colored red), consistent with some of the key structural features observed experimentally by Rodriguez et al.

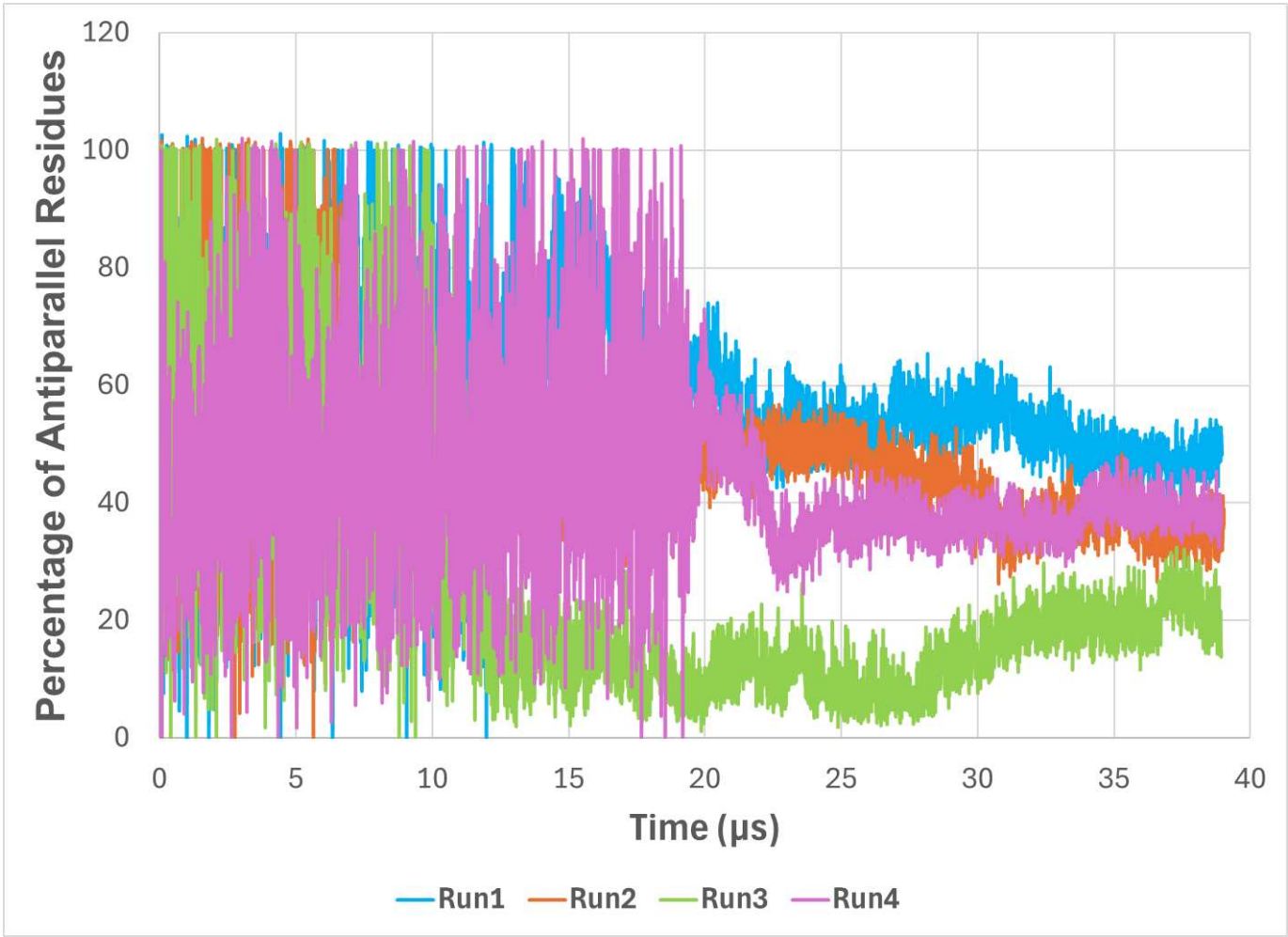

Figure S3 Time evolution of percentage antiparallel residues in P3-WT simulations

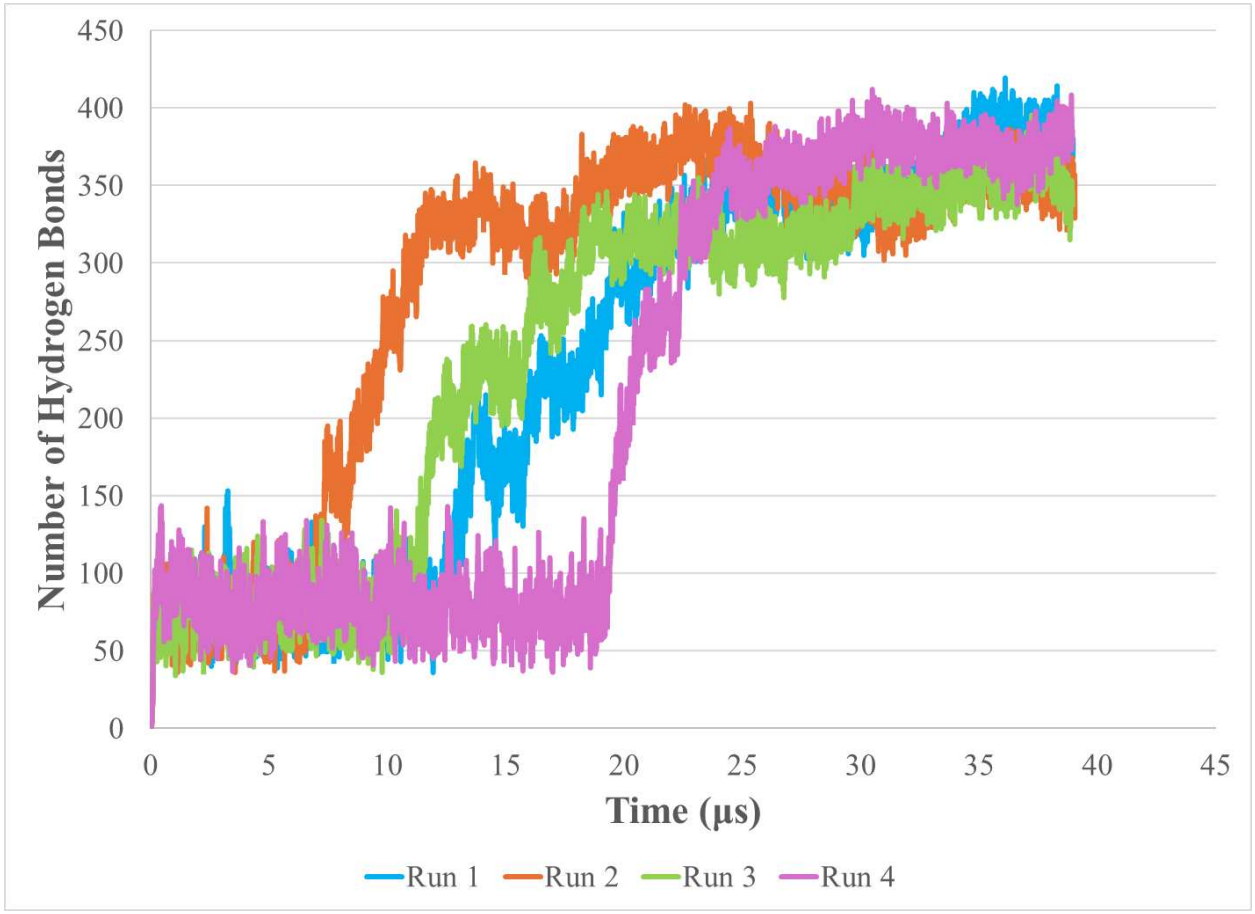

Figure S4 Time evolution of the total number of hydrogen bonds during the four simulations of P3-WT. Each colored plot corresponds to an independent simulation run. At early stage of each simulation, low hydrogen bond formation with fluctuations reflects frequent peptide association and dissociation events. This is followed by a sharp increase in hydrogen bonding as oligomers form. After this, the number of hydrogen bonds keep increasing slowly with fluctuations that indicate fibrillization with local rearrangement and occasional dissociation to reach low energy state conformations.

C1ext: 22 residues – **G_{14}VVAAAEKTKQGVAEAAGKTKE_{35}** 24 chains, C = 10mM, T = 330K		
Run1	Run 2	Run 3
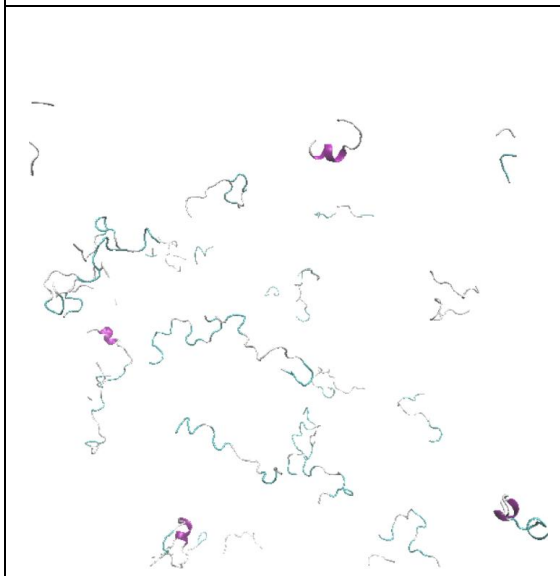	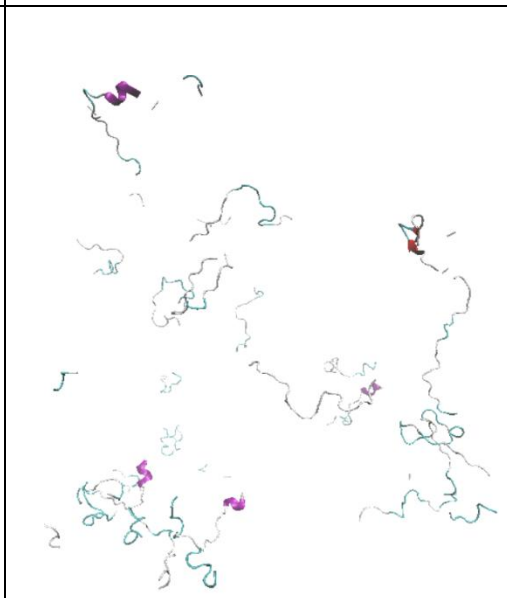	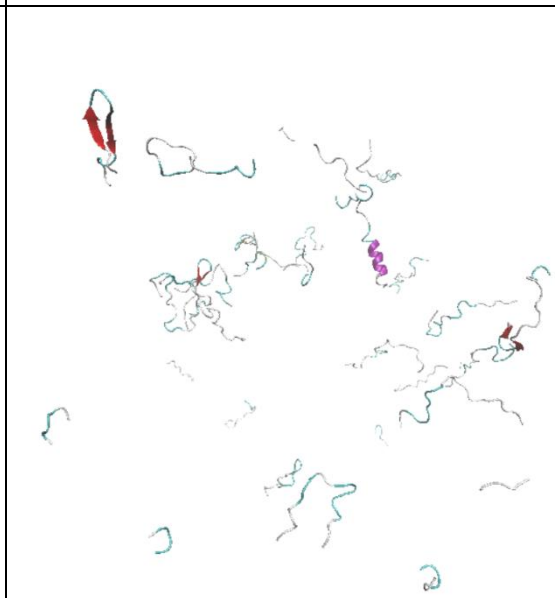

Figure S5 Final snapshots of DMD/PRIME20 simulations of **C1ext**. All simulations didn't aggregate at the end of 500 billion collisions (~38μs)

<table>
<tr><td colspan="4">P3Next-WT: 31 residues – A₂₇EAAGKTKEGVLYVGSKTKEGVVHGVATVAE₅₇
24 chains, C = 10mM, T = 330K</td></tr>
<tr><td>Run 1 – 21% β-hairpins</td><td>Run 2 – 21% β-hairpins</td><td>Run 3 – 22% β-hairpins</td><td></td></tr>
<tr><td>  </td><td> 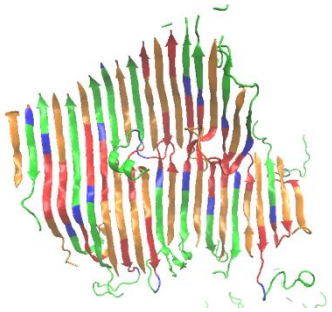 </td><td> 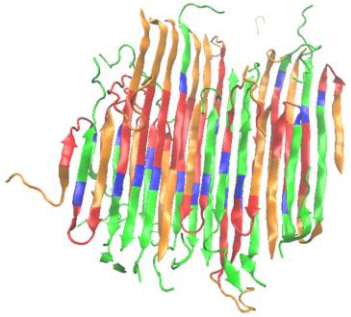 </td><td></td></tr>
<tr><td>Run 4 – 29% β-hairpins</td><td>Run 5 – 21% β-hairpins</td><td>Run 6 – 25%</td><td>Run 7 – 21% β-hairpins</td></tr>
<tr><td> 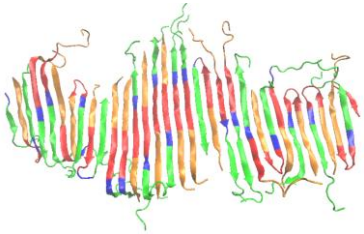 </td><td> 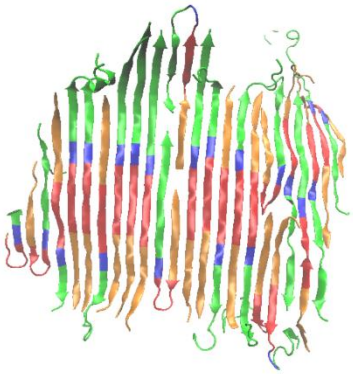 </td><td> 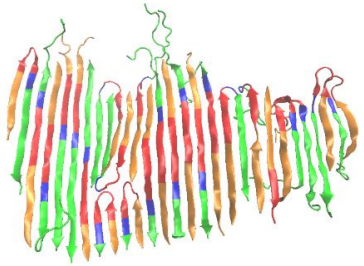 </td><td> 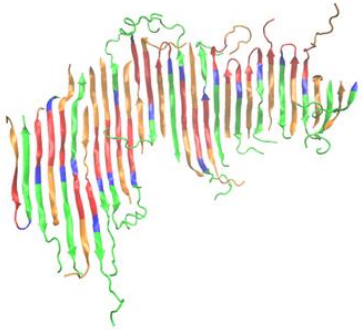 </td></tr>
</table>

Figure S6 Snapshots of final structures of 7 simulations for **P3Next-WT** at 700 billion collisions (~38μs). β-hairpins appear in all fibrils at different percentages

P1: 7 residues - $G_{36}VLYVGS_{42}$ 48 chains, C = 10mM, T = 310K				
	P1-L38M	P1-L38A	P1-V40A	P1-WT
Run1	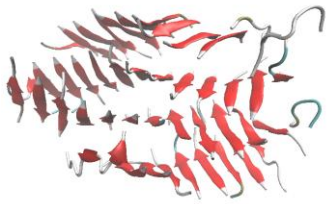	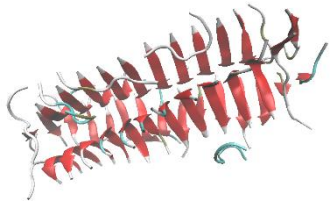		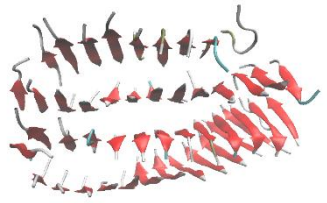
Run2	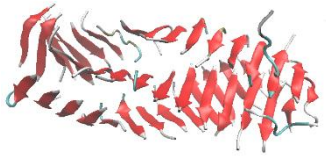	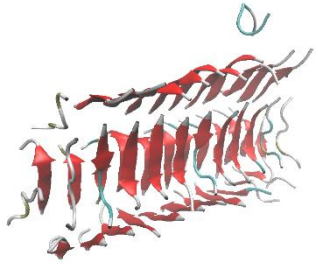		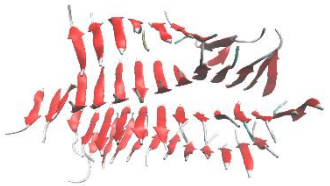
Run3	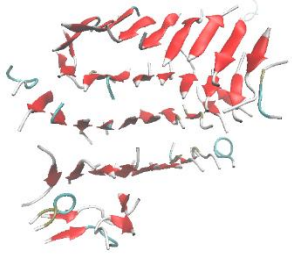	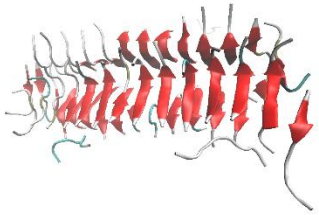	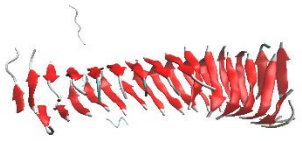	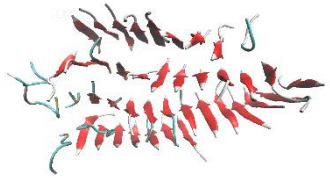

Figure S7 Final snapshots of DMD/PRIME20 simulation of mutated **P1** variants. All snapshots were taken at the end of 300 billion collisions (~31μs)

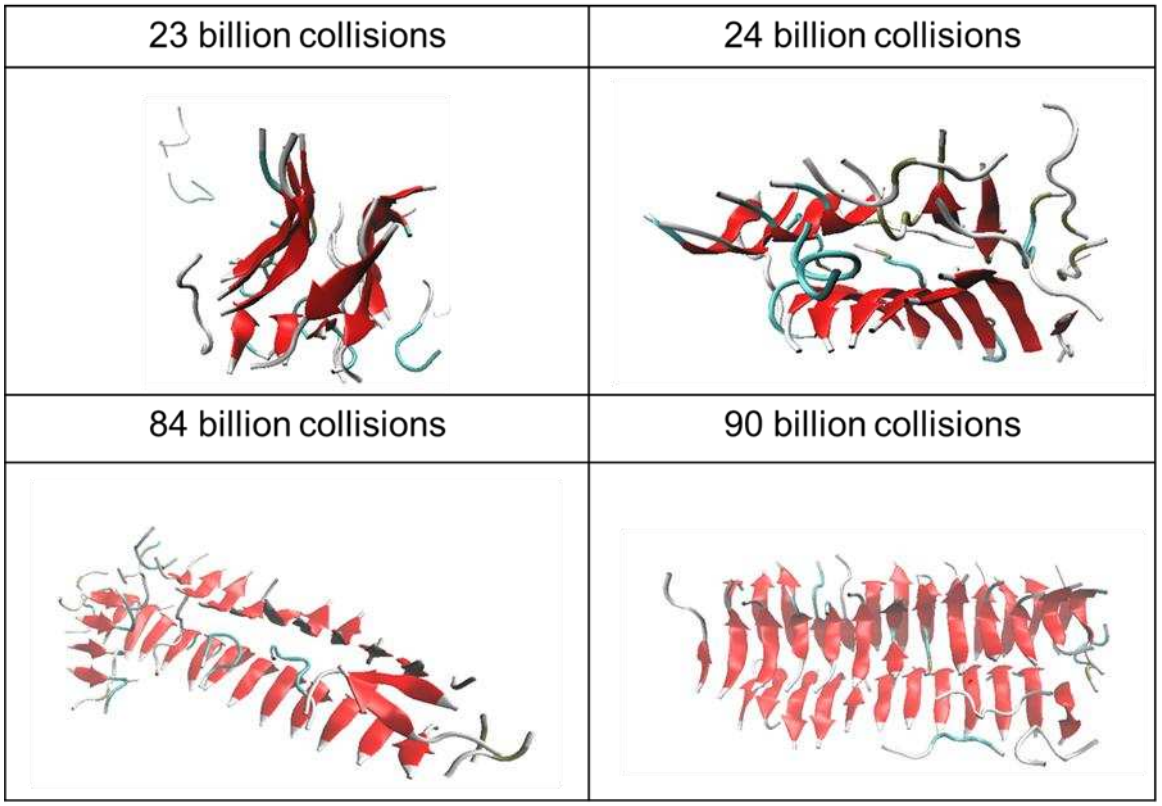

Figure S8 Snapshots at different times during the early stage of fibril formation of **P1-L38A** fragment from one simulation

P3: 22 residues - G_{36}VLYVGSKTKEGVVHGVATVAE_{57} 24 chains, C = 10mM, T = 330K				
	Run 1	Run 2	Run 3	Run 4
L38M	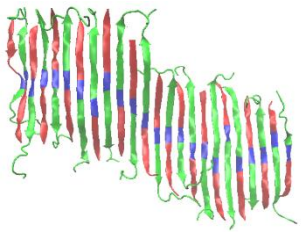	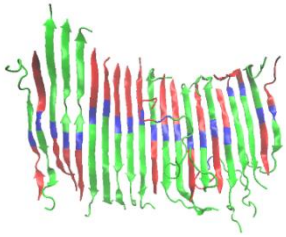	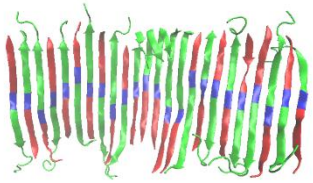	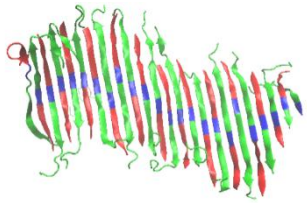
L38A	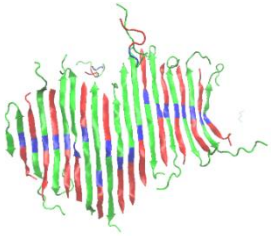	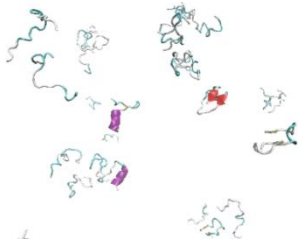	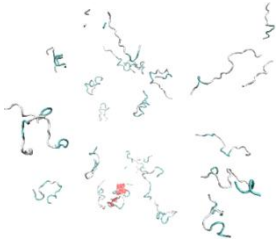	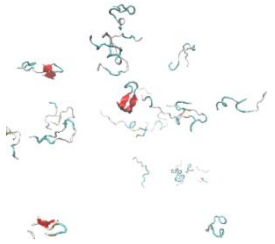
V40A	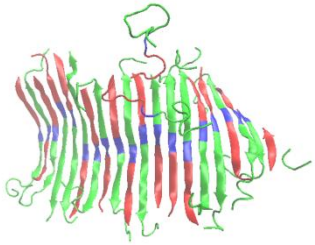		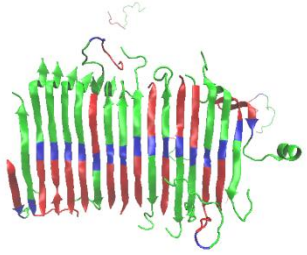	

Figure S9 Final snapshots of DMD/PRIME20 simulation of mutated **P3** variants. All snapshots were taken at the end of 500 billion collisions (~39μs)

<table>
<tr><td colspan="4">P3Next-L38M: 31 residues – A₂₇EAAGKTKEGV<u>M</u>YVGSKTKEGVVHGVATVAE₅₇
24 chains, C = 10mM, T = 330K</td></tr>
<tr><td>Run 1 – 9% β-hairpins</td><td>Run 2 – 21% β-hairpins</td><td>Run 3 – 13% β-hairpins</td><td></td></tr>
<tr><td> 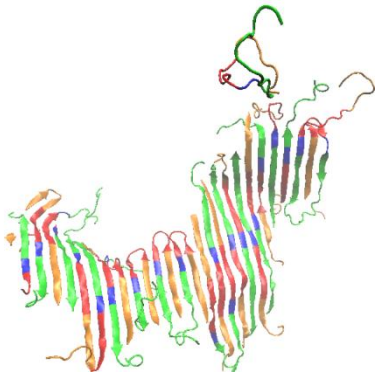 </td><td> 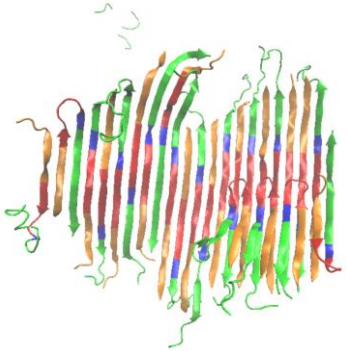 </td><td> 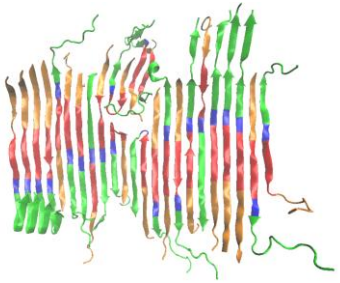 </td><td></td></tr>
<tr><td>Run 4 – 22% β-hairpins</td><td>Run 5 – 17% β-hairpins</td><td>Run 6 – 17% β-hairpins</td><td>Run 7 – 13% β-hairpins</td></tr>
<tr><td> 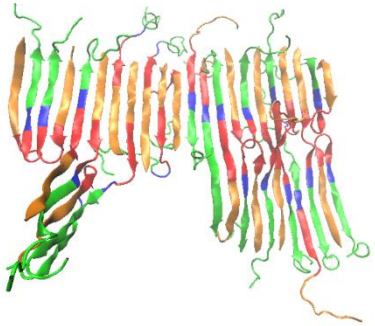 </td><td> 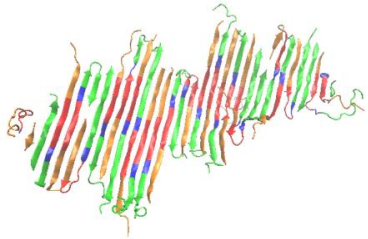 </td><td> 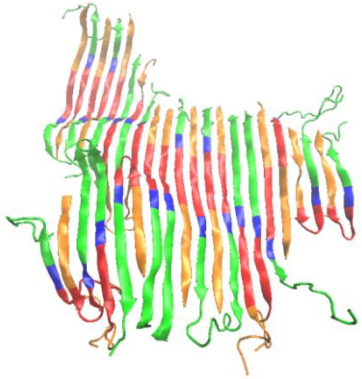 </td><td> 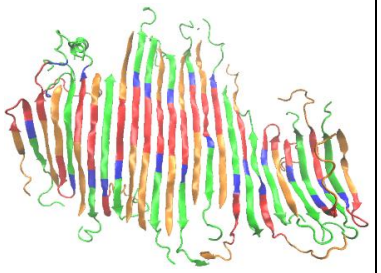 </td></tr>
</table>

Figure S10 Final snapshots of DMD/PRIME20 simulation of mutated **P3Next-L38M** variant at 700 billion collisions (~38μs).

<table>
<tr><td colspan="4">P3Next-L38A: 31 residues – A₂₇EAAGKTKEGV<u>A</u>YVGSKTKEGVVHGVATVAE₅₇
24 chains, C = 10mM, T = 330K</td></tr>
<tr><td>Run 1 – 60% β-hairpins</td><td>Run 2 – 33% β-hairpins</td><td>Run 3</td><td></td></tr>
<tr><td> 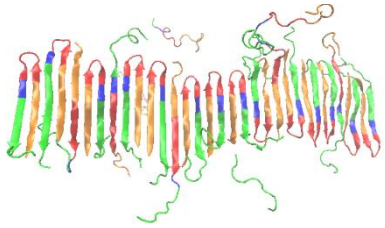 </td><td> 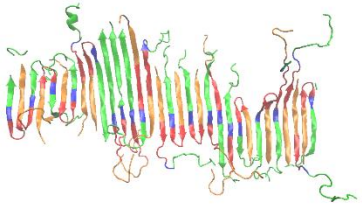 </td><td> 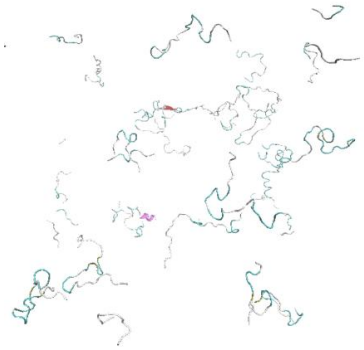 </td><td></td></tr>
<tr><td>Run 4 – 47% β-hairpins</td><td>Run 5</td><td>Run 6 – 67% β-hairpins</td><td>Run 7 – 21% β-hairpins</td></tr>
<tr><td> 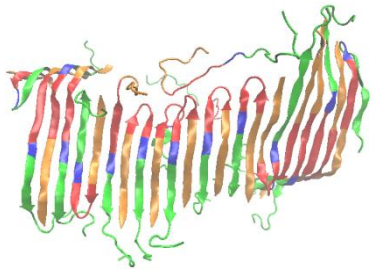 </td><td> 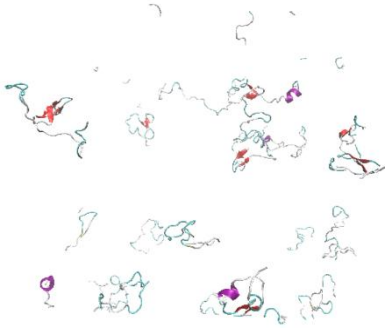 </td><td> 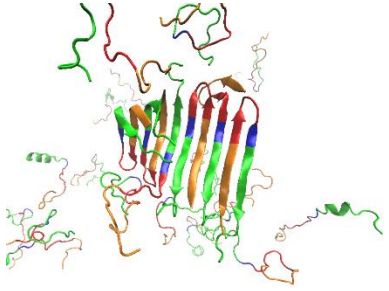 </td><td> 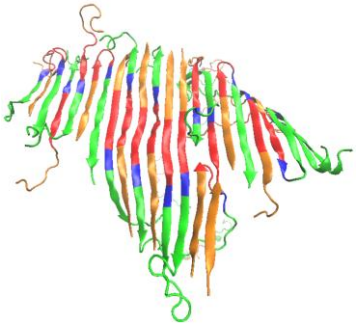 </td></tr>
</table>

Figure S11 Final snapshots of DMD/PRIME20 simulation of mutated **P3Next-L38A** variant at 700 billion collisions (~38μs).

<table>
<tr><td colspan="4">P3Next-V40A: 31 residues – A₂₇EAAGKTKEGVLY<u>A</u>GSKTKEGVVHGVATVAE₅₇
24 chains, C = 10mM, T = 330K</td></tr>
<tr><td>Run 1 – 41% β-hairpins</td><td>Run 2</td><td>Run 3– 64% β-hairpins</td><td></td></tr>
<tr><td> 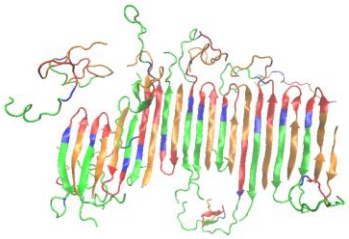 </td><td> 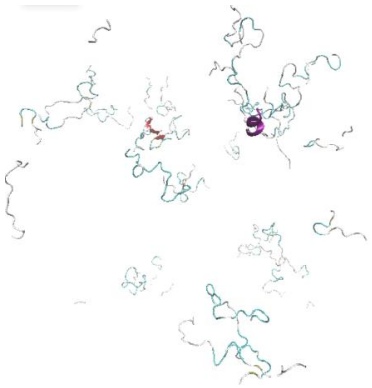 </td><td> 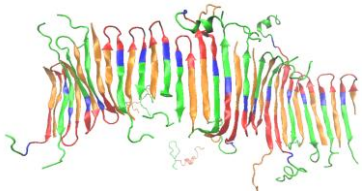 </td><td></td></tr>
<tr><td>Run 4 – 44% β-hairpins</td><td>Run 5 – 24% β-hairpins</td><td>Run 6 – 27% β-hairpins</td><td>Run 7 – 18% β-hairpins</td></tr>
<tr><td> 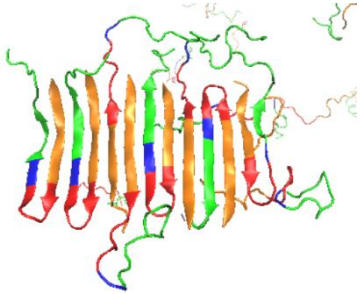 </td><td> 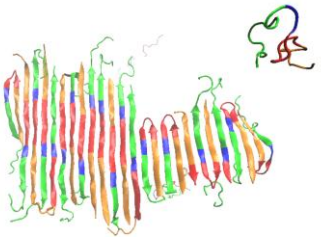 </td><td> 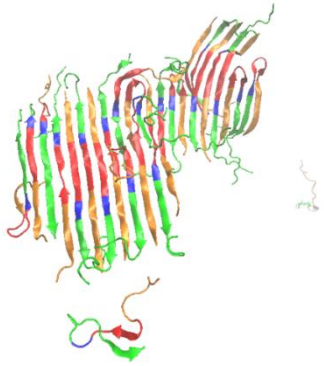 </td><td> 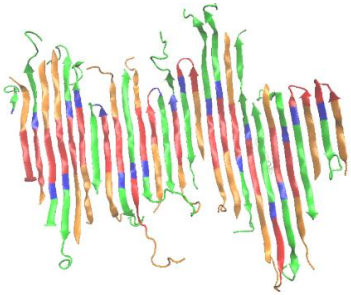 </td></tr>
</table>

Figure S12 Final snapshots of DMD/PRIME20 simulation of mutated **P3Next-V40A** variant at 700 billion collisions (~38μs).

P3-L38A-Run2	P3-L38A-Run3	P3-L38A-Run4
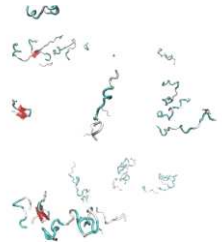		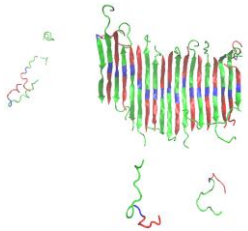
P3-V40A-Run2	P3-V40A-Run4	
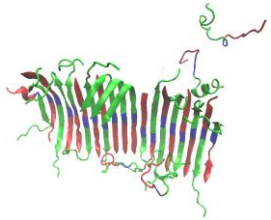	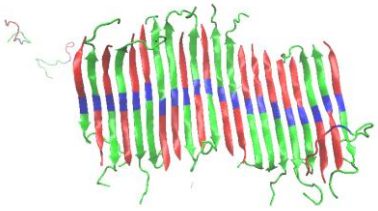	
P3Next-L38A-Run3	P3Next-L38A-Run5	P3Next-V40A-Run2
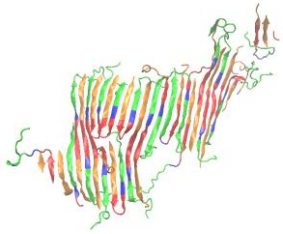	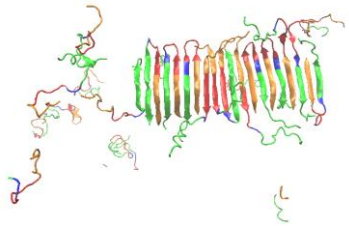	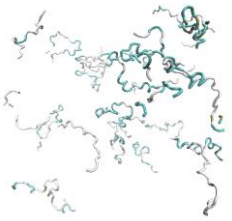

Figure S13 Final snapshots from kinetic-trap testing simulations for non-aggregating samples from the original simulations. The figure includes three simulations of P3-L38A (first row), two simulations of P3-V40A (second row), two simulations of P3Next-L38A (first panel and second panel on the third row), and one simulation of P3Next-V40A (third panel on the third row). Panels show the outcomes after heating, annealing back to 330K and simulating for 500 billion collisions. Runs that form β-sheets indicate that the system has escaped from kinetic traps and that the kinetic trap was the reason for these systems not being able to aggregate. The runs that remain disordered suggest that thermodynamic property changes associated with the mutations might be the reason for these systems not being able to aggregate.

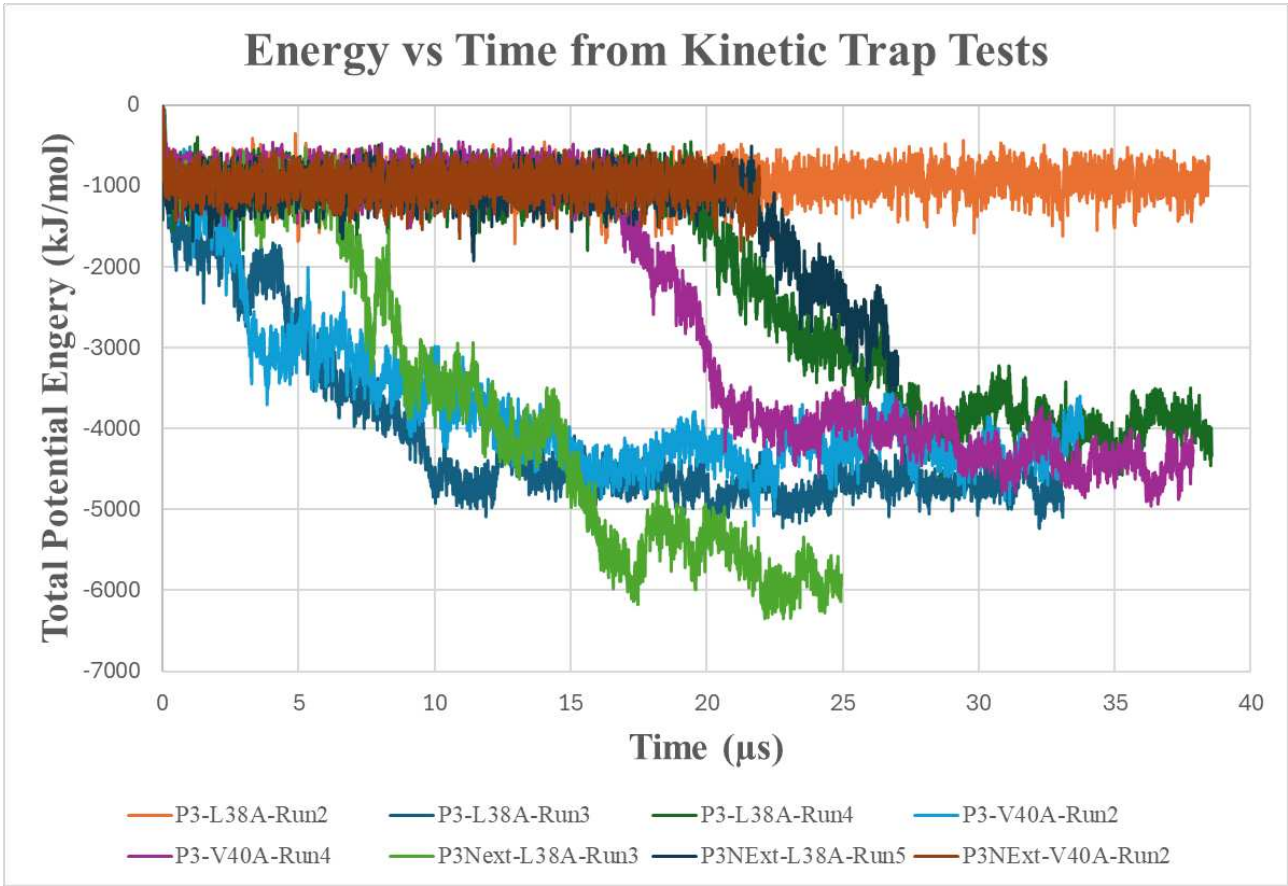

Figure S14 Total potential energy vs. time for kinetic-trap tests of non-aggregating samples of P3 and P3Next-L38A and V40A. Each sample was subjected to a brief temperature increase followed by annealing to the original simulation temperature of 330K. Thereafter they were simulated for 500 billion collisions to test whether the runs in which the peptides did not aggregate were kinetically trapped or thermodynamically unfavorable. Runs that exhibit a large decrease in potential energy after the perturbation indicate that their original failures to aggregate arose from kinetic trapping. In contrast, runs that remain at high energy suggest mutation-dependent thermodynamic property change.

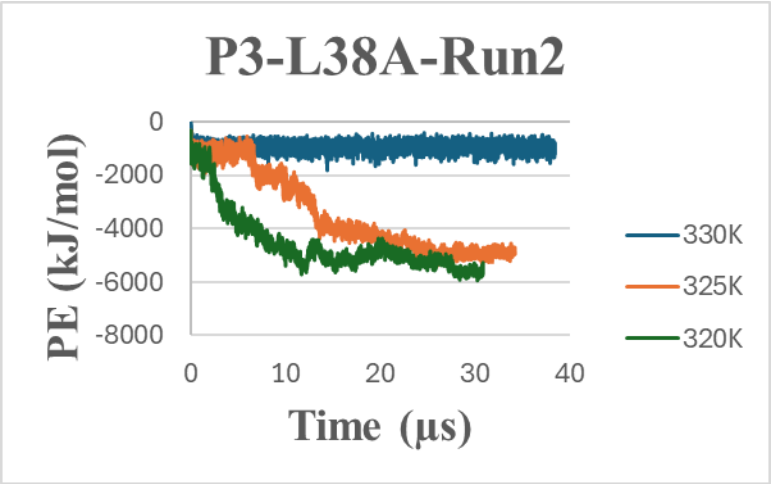

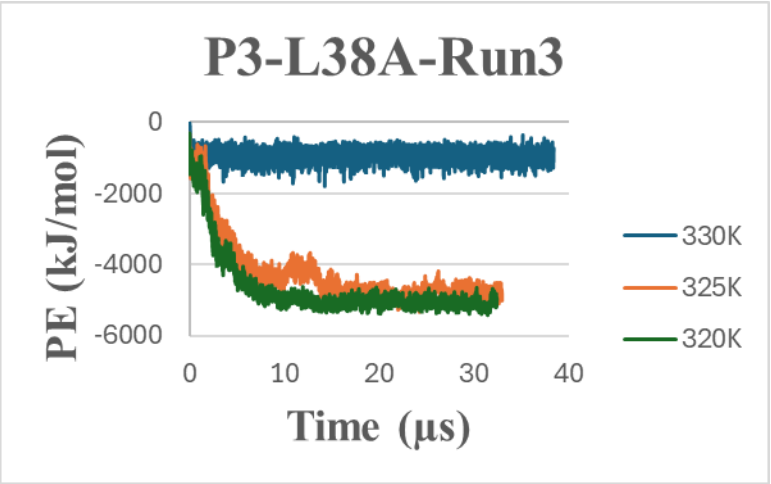

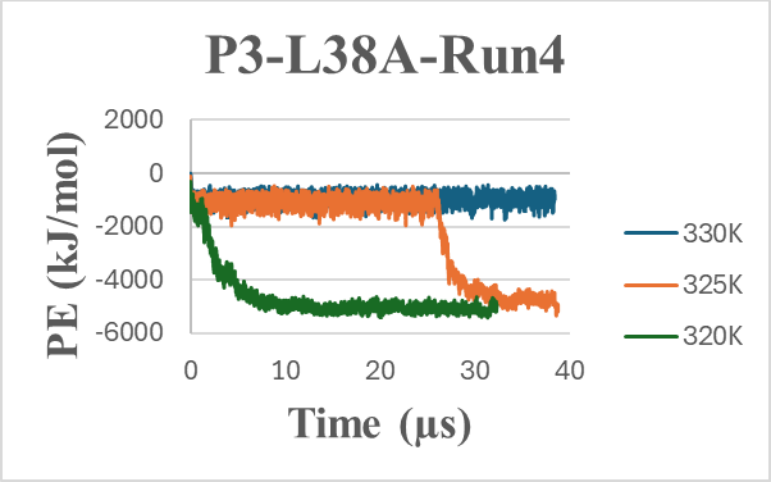

T	325K	320K
Run2	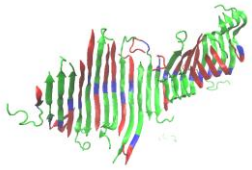	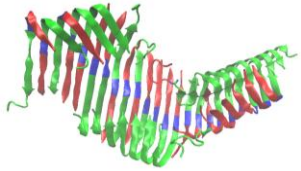
Run3	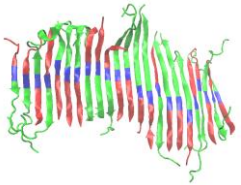	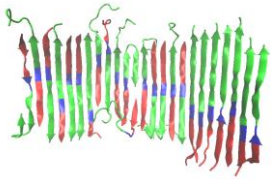
Run4	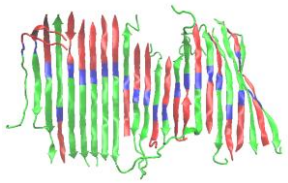	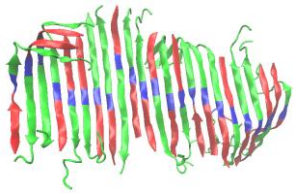

Figure S15 Potential energy vs. time and final snapshots for non-aggregating P3-L38A (at 330 K) simulated at 325 K, and 320 K.

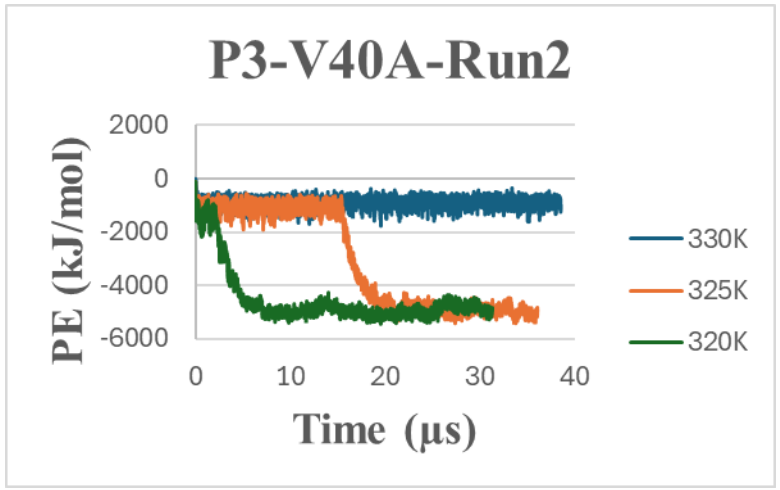

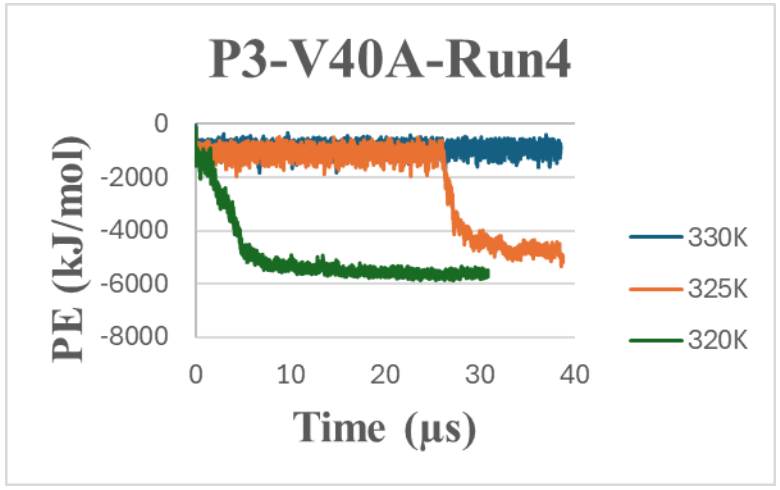

T	325K	320K
Run2	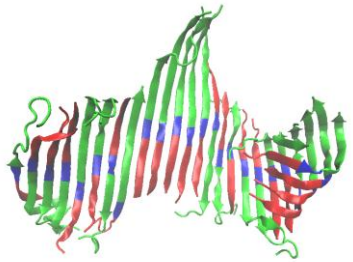	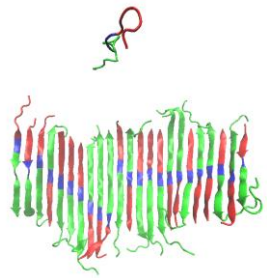
Run4	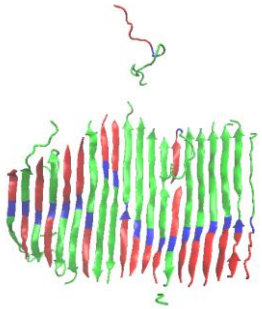	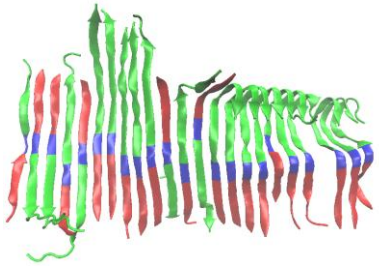

Figure S16 Potential energy vs. time and final snapshots for non-aggregating P3-V40A (at 330 K) simulated at 325 K, and 320 K.

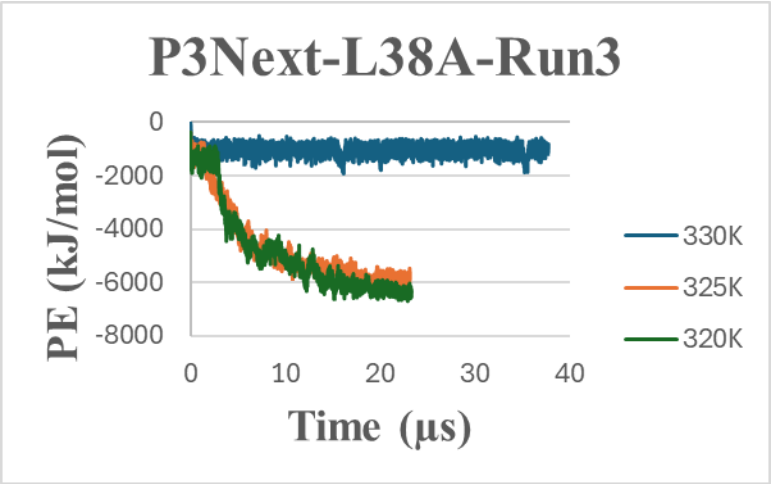

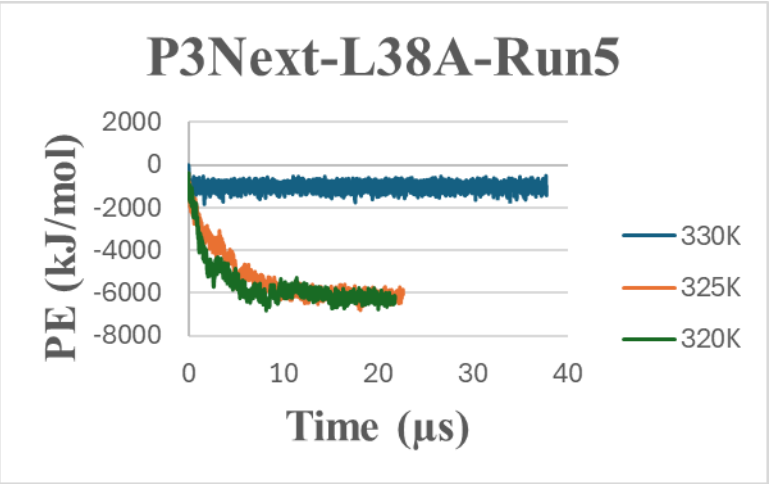

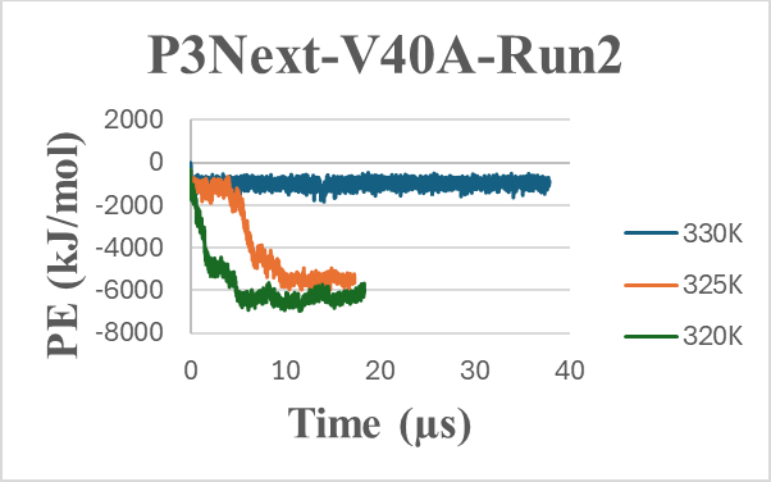

Figure S17 Potential energy vs. time and final snapshots for non-aggregating P3Next-L38A and -V40A (at 330 K) simulated at 325 K, and 320 K.

T	325K	320K
P3Next-L38A Run3	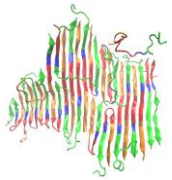	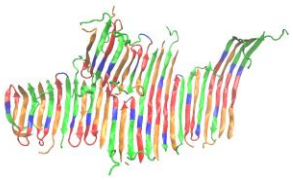
P3Next-L38A Run5	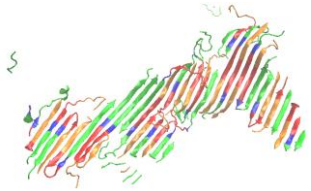	
P3Next-V40A Run2	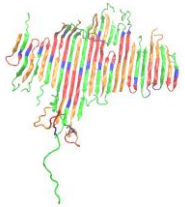	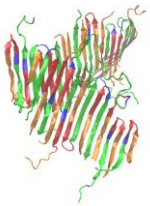

P1: 7 residues - **$G_{36}VLYVGS_{42}$** 48 chains, C = 10mM, T = 310K		
	P1-Y39A	P1-S42A
Run1		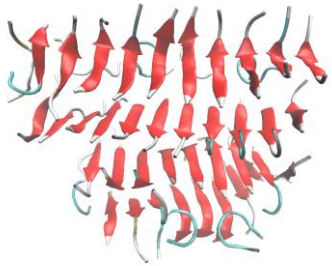
Run2	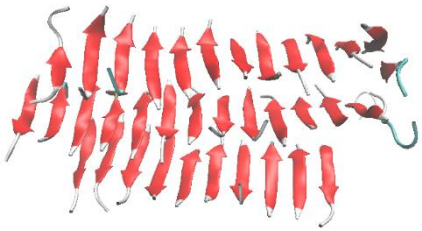	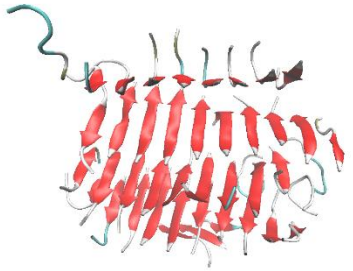
Run3	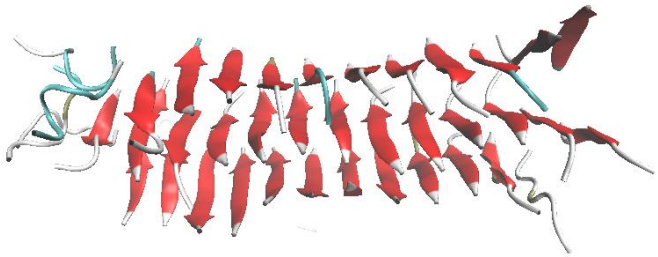	

Figure S18 Final snapshots of DMD/PRIME20 simulation of mutated **P1-Y39A** and **-S42A**. All snapshots were taken at the end of 300 billion collisions (~31μs)

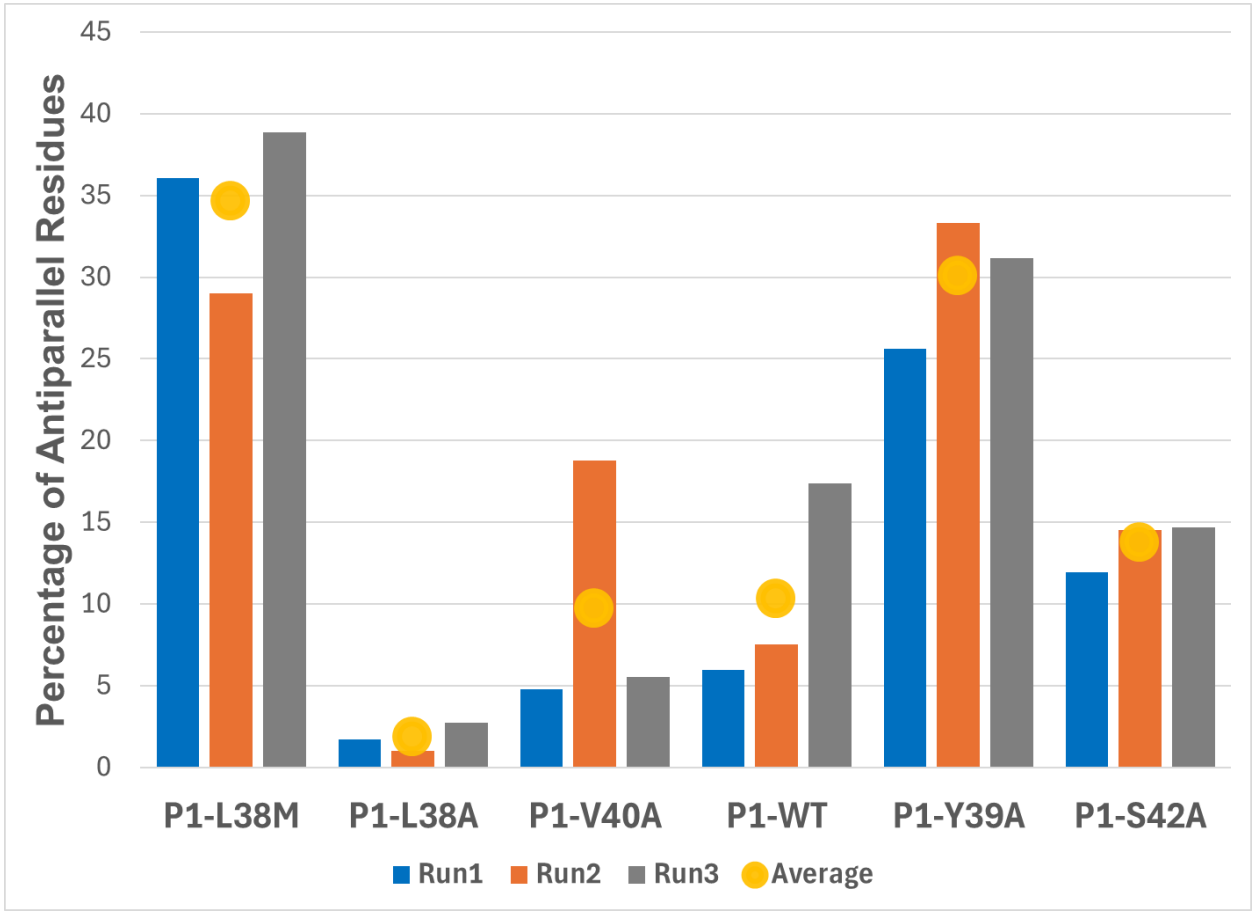

Figure S19 Average percentage of β-sheet residues adopting an antiparallel arrangement within the fibrillar structures of all simulated peptide variants

P3Next-Y39A: 31 residues – A$_{27}$EAAGKTKEGVL*A*VGSKTKEGVVHGVATVAE$_{57}$ 24 chains, C = 10mM, T = 330K			
Run 1 – 39% β-hairpins	Run 2 - 29% β-hairpins	Run 3 – 32% β-hairpins	
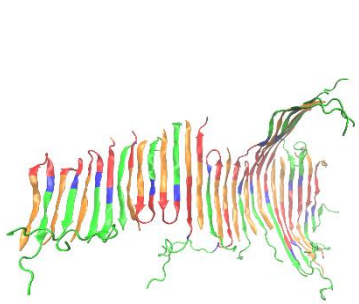			
Run 4 – 35% β-hairpins	Run 5 – 41% β-hairpins	Run 6 – 17% β-hairpins	Run 7 – 21% β-hairpins
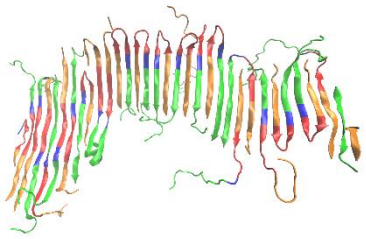	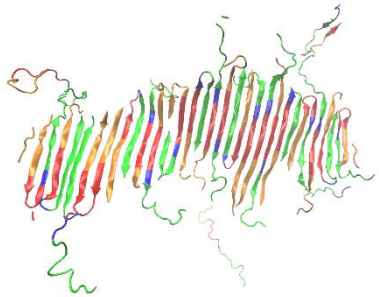	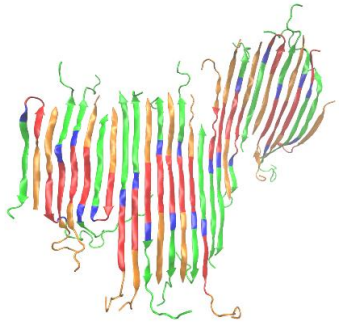	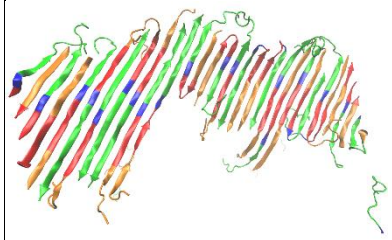

Figure S20 Final snapshots of DMD/PRIME20 simulation of mutated **P3Next-Y39A** variant at 700 billion collisions (~38μs).

P3Next-S42A: 31 residues – A27EAAGKTKEGVLYVGAKTKEGVVHGVATVAE57 24 chains, C = 10mM, T = 330K			
Run 1 – 32% β-hairpins	Run 2 - 14% β-hairpins	Run 3 – 18% β-hairpins	
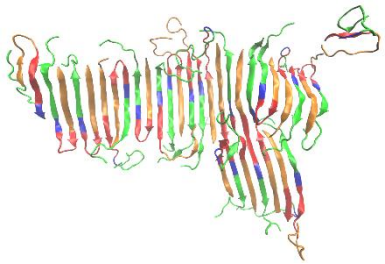	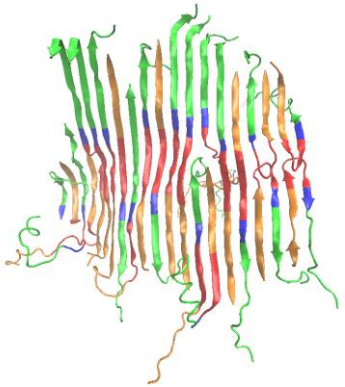	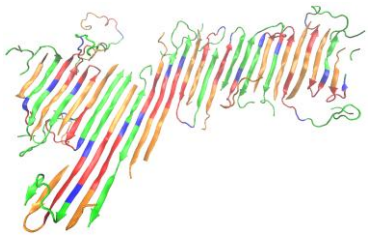	
Run 4 – 21% β-hairpins	Run 5 – 38% β-hairpins	Run 6 – 17% β-hairpins	Run 7 – 25% β-hairpins
		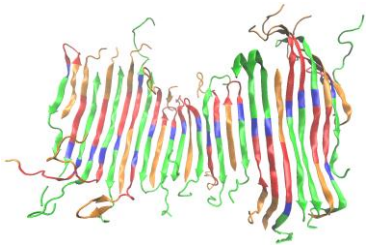	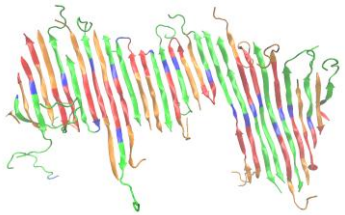

Figure S21 Final snapshots of DMD/PRIME20 simulation of mutated **P3Next-S42A** variant at 700 billion collisions (~38μs).

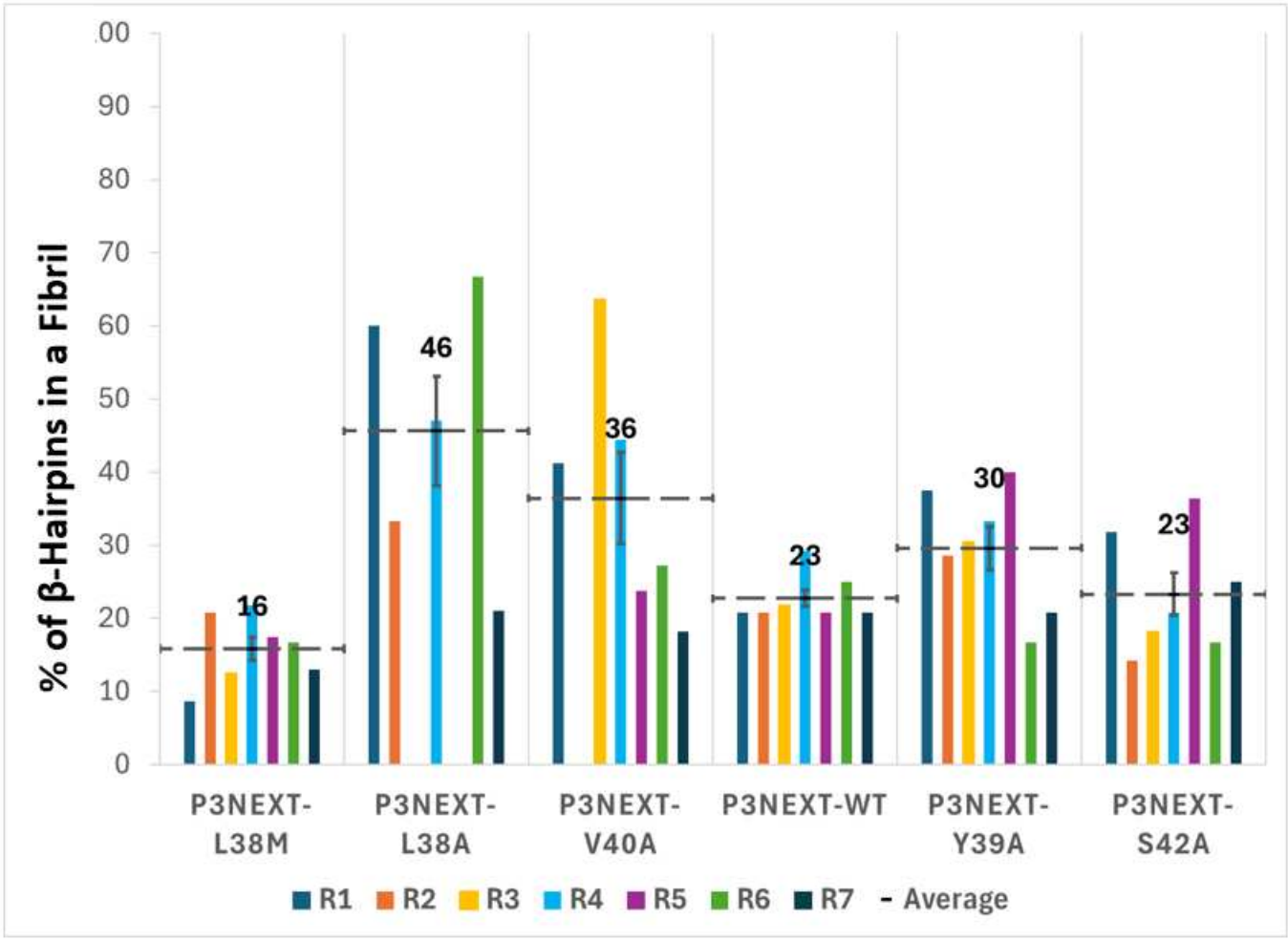

Figure S22 Average percentage of β-hairpin structures formed within fibrils across all simulated peptide variants

<table>
<tr><th colspan="3">Fibril structure from PRIME20 simulation (red arrows)
And from PULCHRA backmapping algorithm (atoms)</th></tr>
<tr><td colspan="3"> 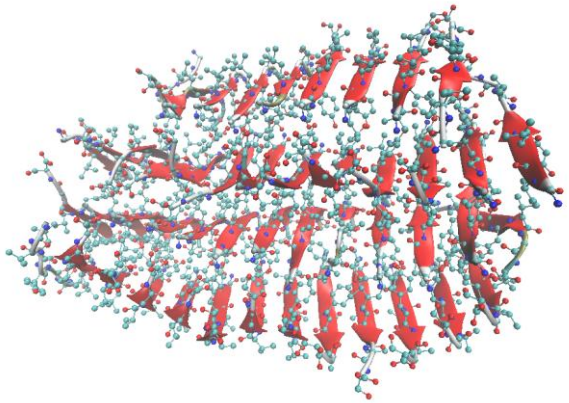 </td></tr>
<tr><th>MD Run1</th><th>MD Run 2</th><th>MD Run 3</th></tr>
<tr><td> 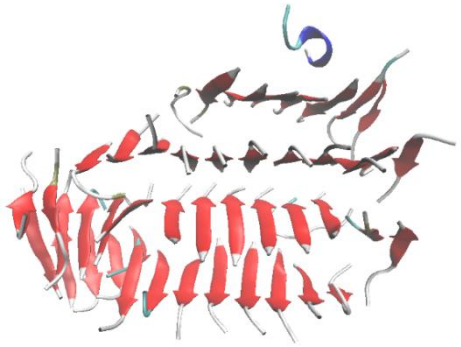 </td><td> 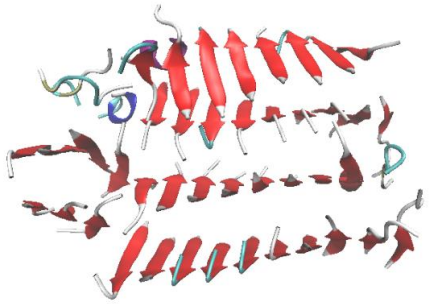 </td><td> 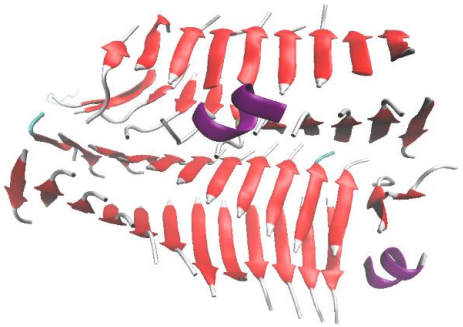 </td></tr>
</table>

Figure S23 Comparison of fibril structures obtained from PRIME20 simulations and atomistic MD simulations. Top: fibril conformation generated from DMD/PRIME20 simulation of P1-WT-Run1 (red arrows) and the corresponding all-atom structure reconstructed using the PULCHRA back-mapping algorithm. Bottom: final fibril conformations from three independent 500ns atomistic MD simulations (Run 1–3) initiated from the backmapped structure. The three trajectories show consistent preservation of the parallel β-sheet conformations with variations in local strand registry and formation of helices.

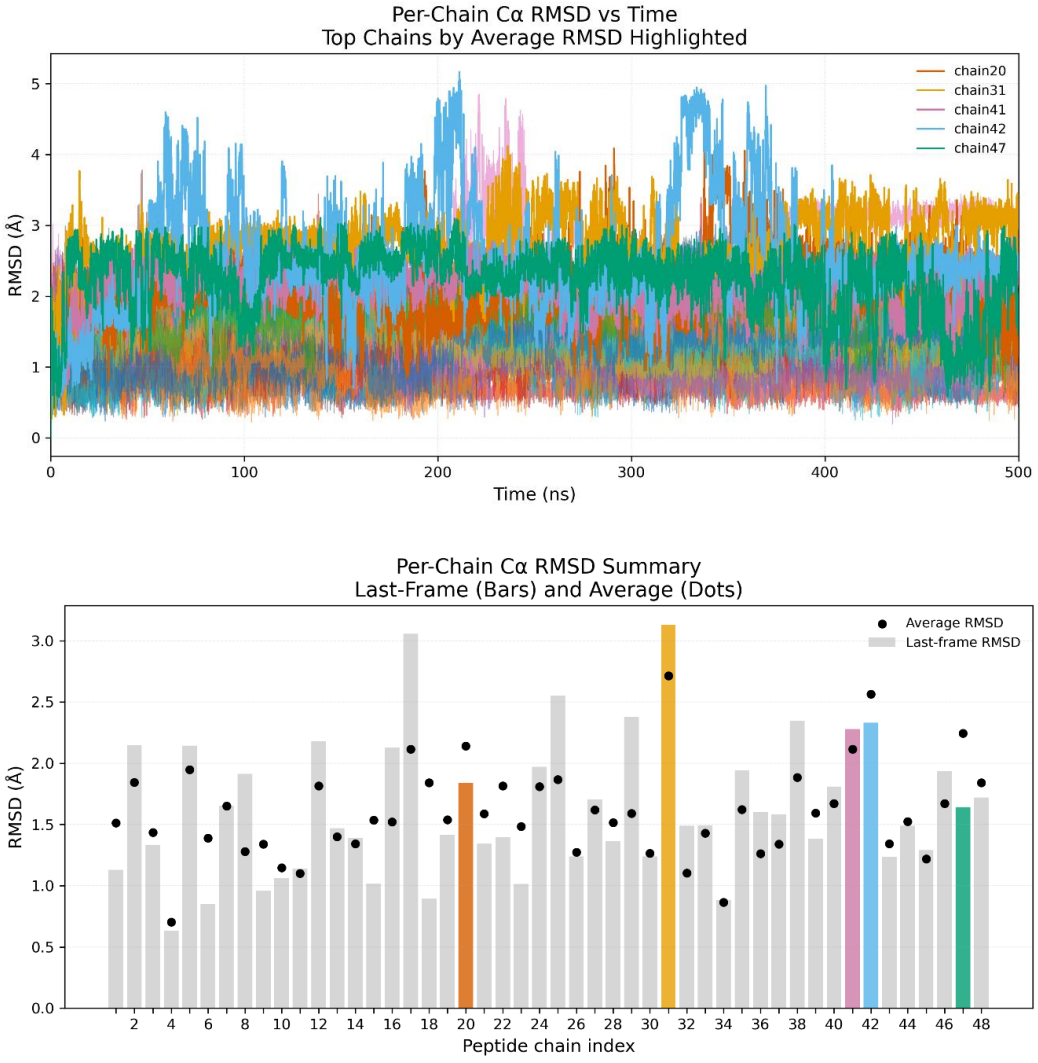

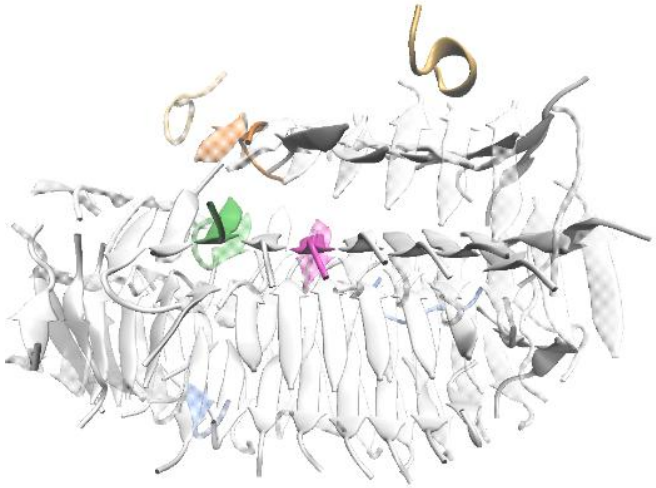

Figure S24 Per-chain structural stability analysis of P1WT fibril during MD Run 1. Top left: time evolution of Cα RMSD for all 48 peptide chains over a 500ns MD simulation. The five chains with the highest average RMSD are labeled while all others are shown in light traces. Top right: structural visualization of the fibril with the same five highest RMSD chains colored to indicate their changes. Initial structure is transparent while final structure is solid. Bottom: summary of per-chain RMSD values. Bars show the last frame while black dots indicate the average RMSD over the trajectory. Colored bars correspond to the highlighted chains in the time evolution plot.

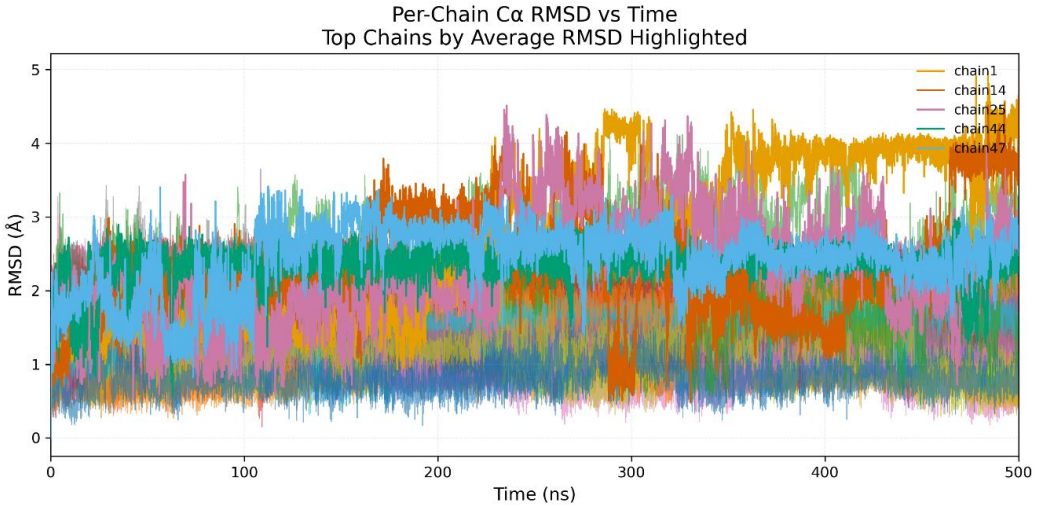

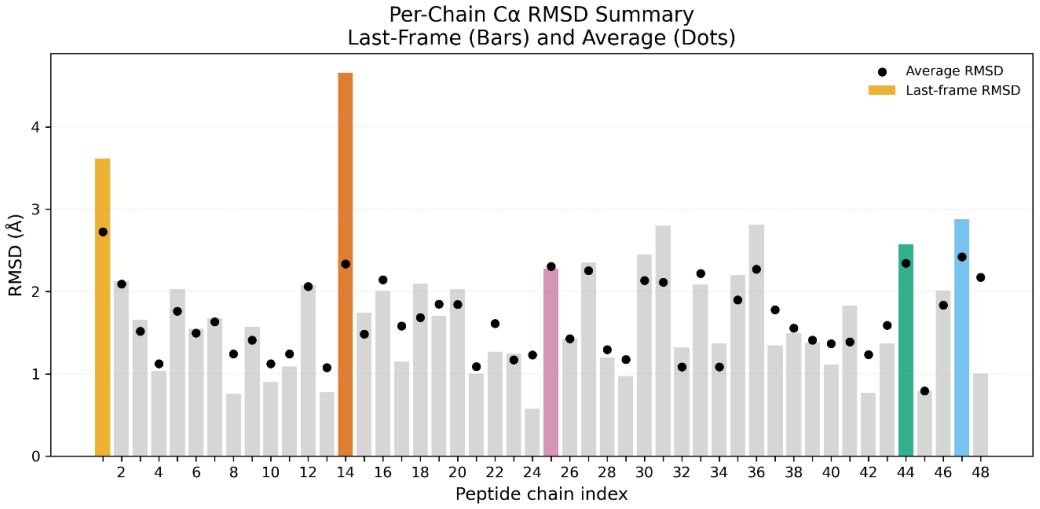

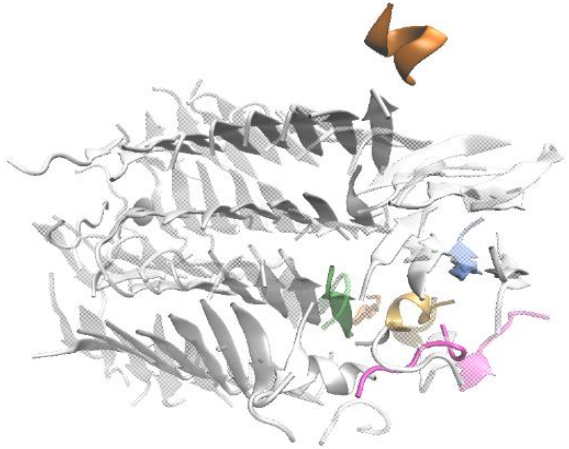

Figure S25 Per-chain structural stability analysis of P1WT fibril during MD Run 2. Top left: time evolution of Cα RMSD for all 48 peptide chains over a 500ns MD simulation. The five chains with the highest average RMSD are labeled while all others are shown in light traces. Top right: structural visualization of the fibril with the same five highest RMSD chains colored to indicate their changes. Initial structure is transparent while final structure is solid. Bottom: summary of per-chain RMSD values. Bars show the last frame while black dots indicate the average RMSD over the trajectory. Colored bars correspond to the highlighted chains in the time evolution plot.

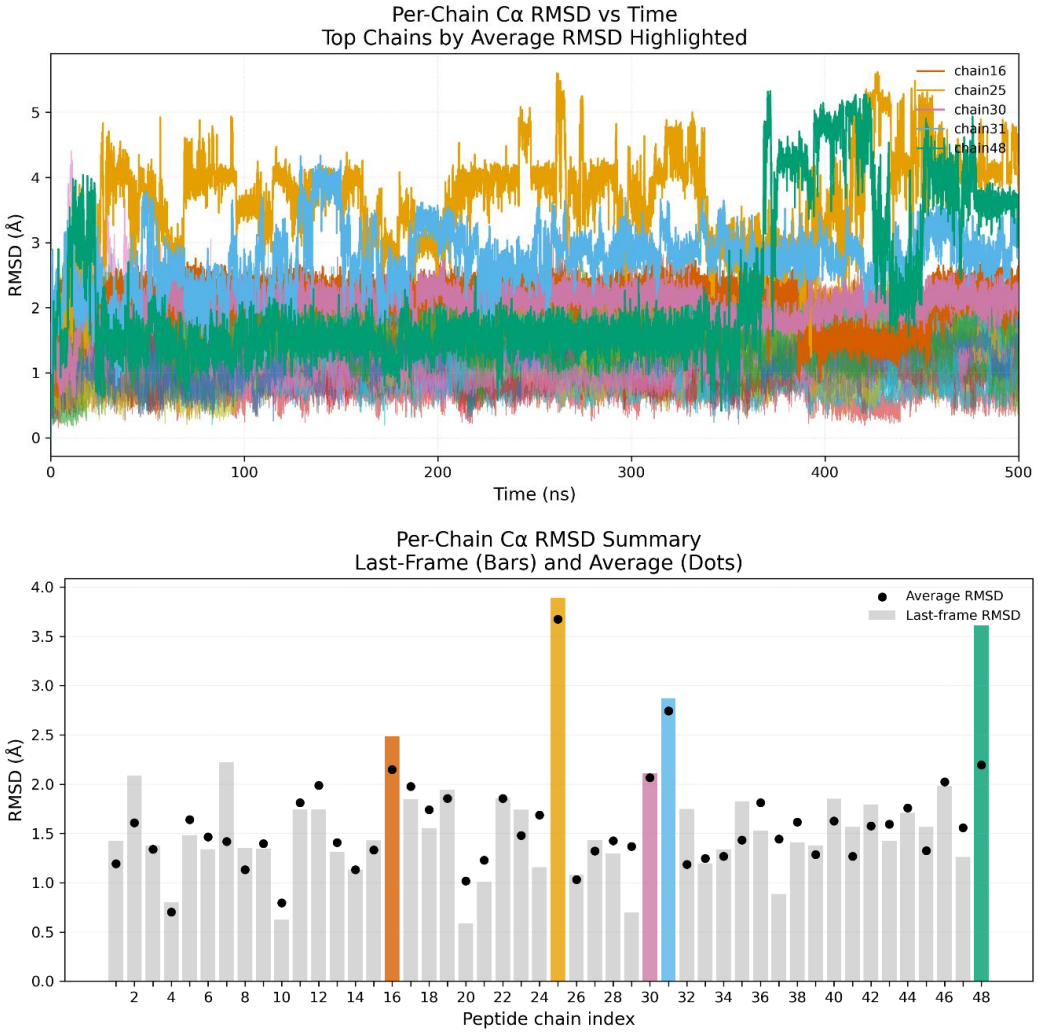

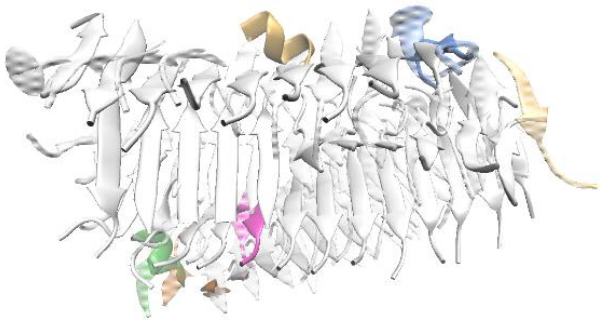

Figure S26 Per-chain structural stability analysis of P1WT fibril during MD Run 3. Top left: time evolution of Cα RMSD for all 48 peptide chains over a 500ns MD simulation. The five chains with the highest average RMSD are labeled while all others are shown in light traces. Top right: structural visualization of the fibril with the same five highest RMSD chains colored to indicate their changes. Initial structure is transparent while final structure is solid. Bottom: summary of per-chain RMSD values. Bars show the last frame while black dots indicate the average RMSD over the trajectory. Colored bars correspond to the highlighted chains in the time evolution plot.

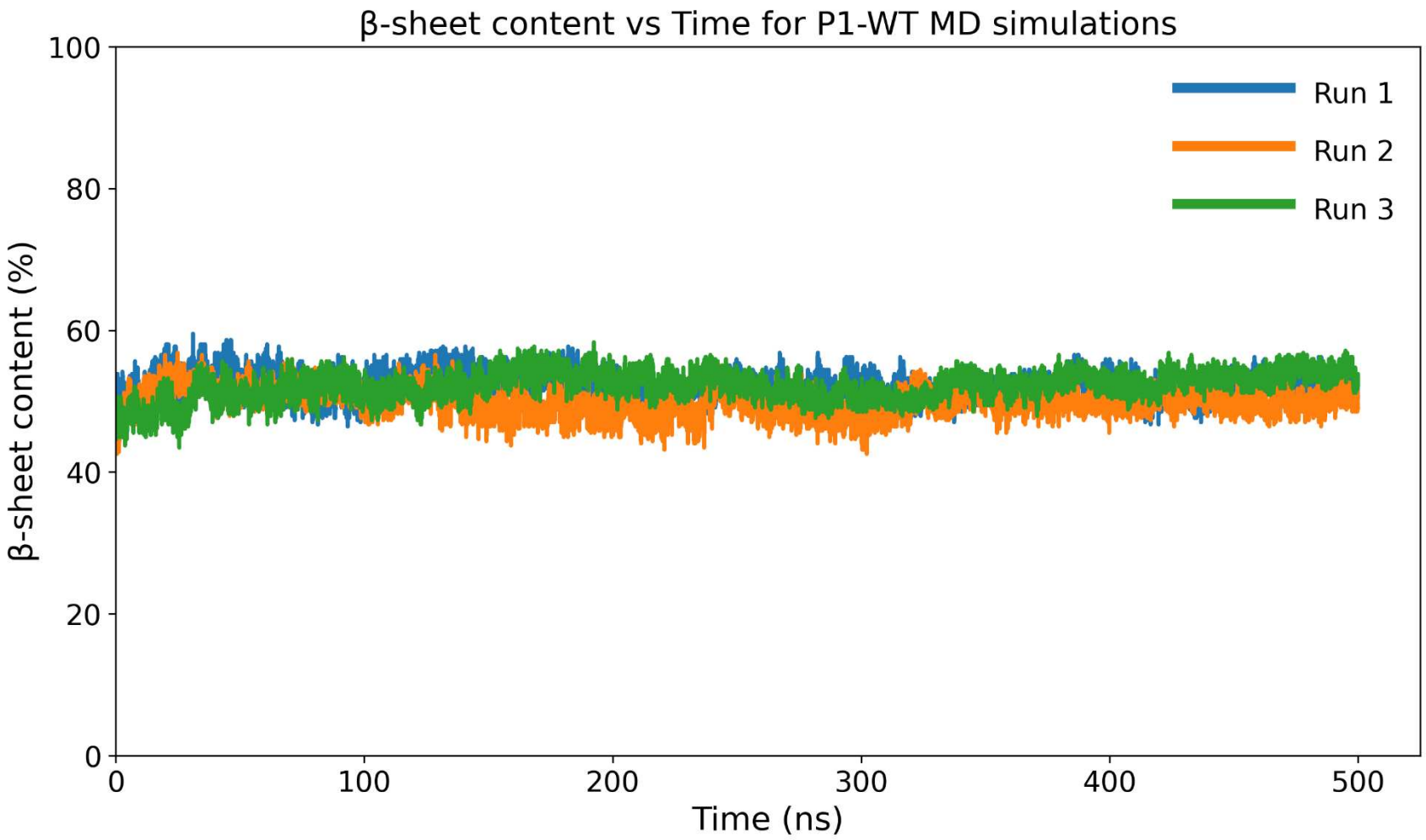

Figure S27 Time evolution of β-sheet content across three independent MD simulations of atomistic-resolution P1-WT fibril reconstructed from DMD/PRIME20 simulation.

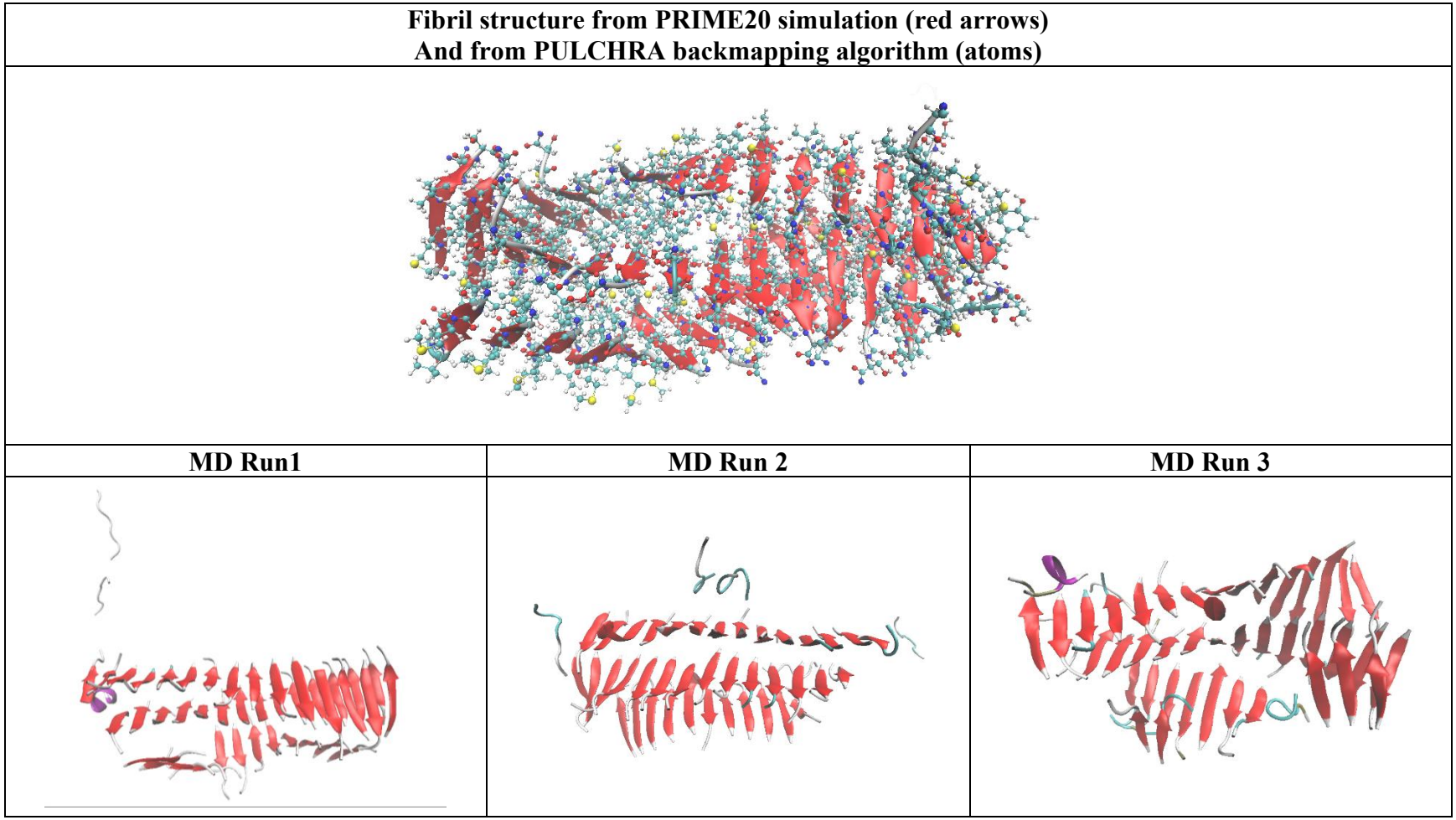

Figure S28 Comparison of fibril structures obtained from PRIME20 simulations and atomistic MD simulations. Top: fibril conformation generated from DMD/PRIME20 simulation of P1-L38M-Run2 (red arrows) and the corresponding all-atom structure reconstructed using the PULCHRA back-mapping algorithm. Bottom: *f*inal fibril conformations from three independent 5*0*0ns atomistic MD simulations (Run 1–3) initiated from the backmapped structure. The three trajectories show consistent preservation of the parallel β-sheet conformations with variations in local strand registry and appearance of monomers dissociated from the fibril.

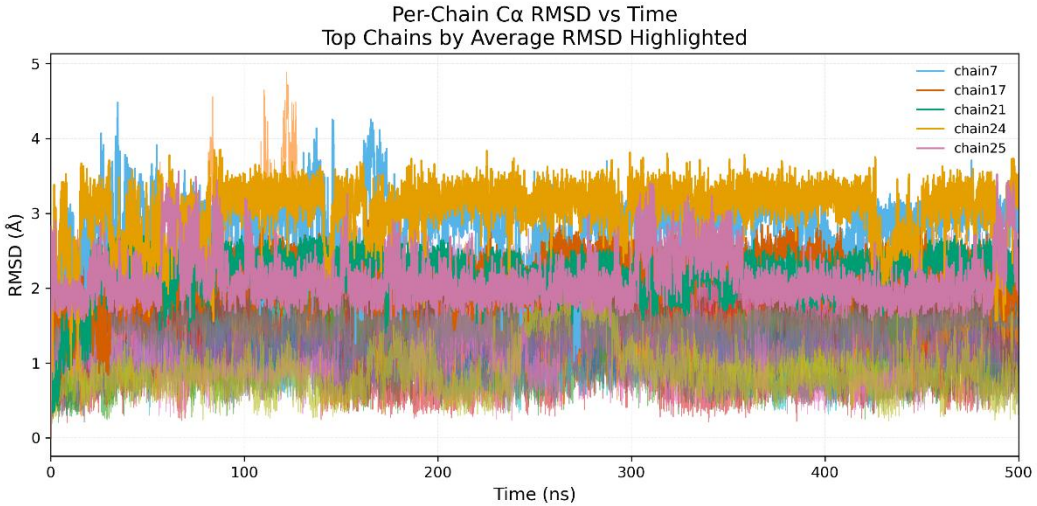

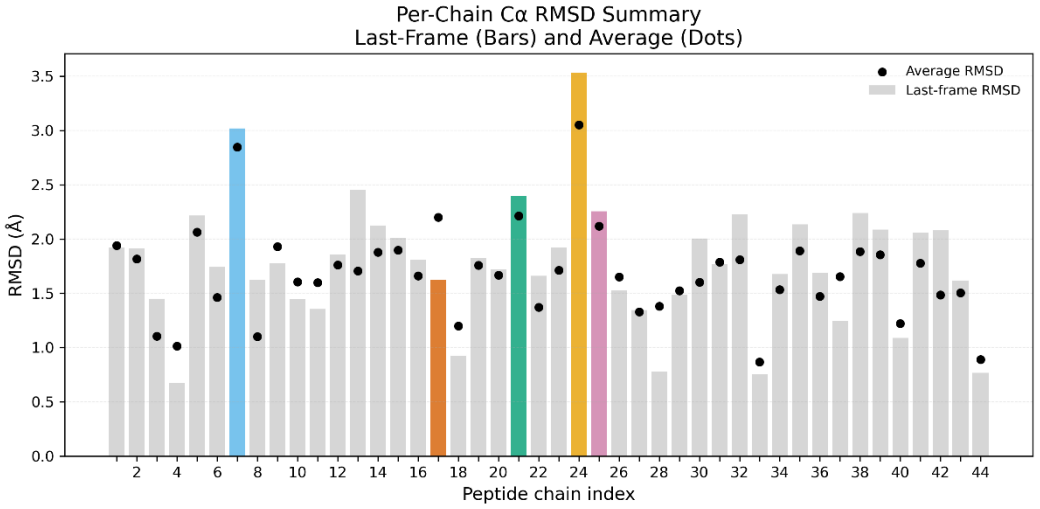

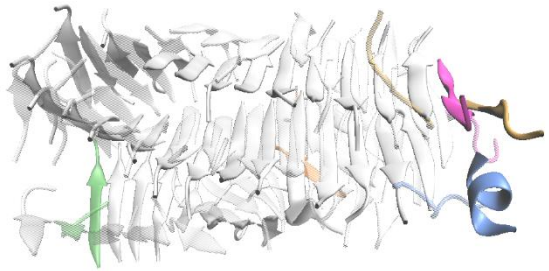

Figure S29 Per-chain structural stability analysis of P1-L38M fibril during MD Run 1. Top left: time evolution of Cα RMSD for all 44 peptide chains over a 500ns MD simulation. The five chains with the highest average RMSD are labeled while all others are shown in light traces. Top right: structural visualization of the fibril with the same five highest RMSD chains colored to indicate their changes. Initial structure is transparent while final structure is solid. Bottom: summary of per-chain RMSD values. Bars show the last frame while black dots indicate the average RMSD over the trajectory. Colored bars correspond to the highlighted chains in the time evolution plot.

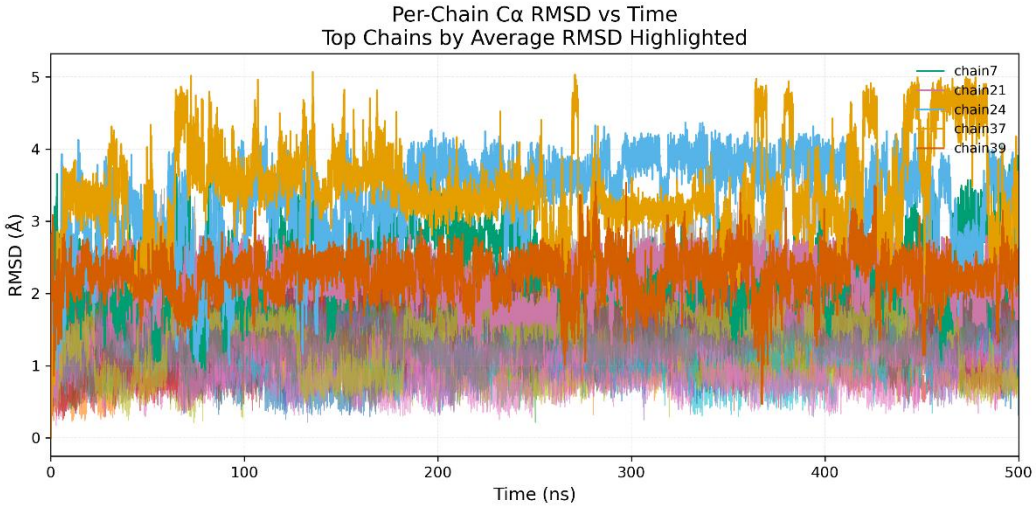

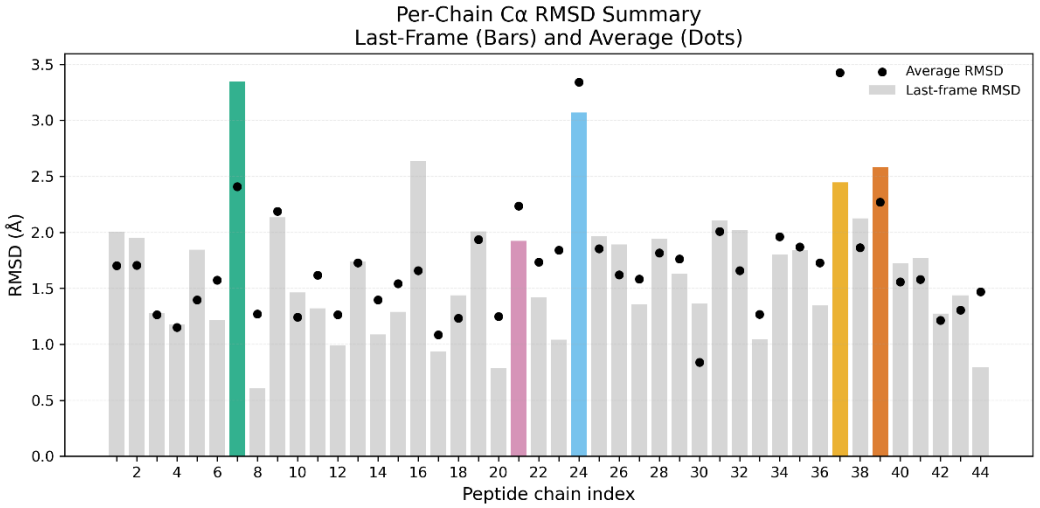

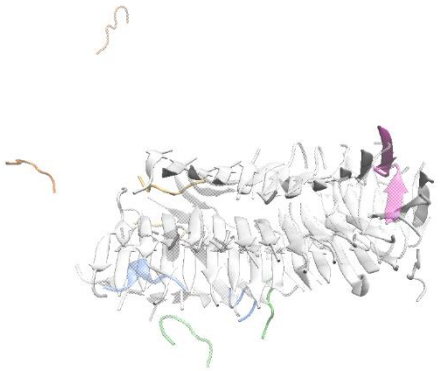

Figure S30 Per-chain structural stability analysis of P1-L38M fibril during MD Run 2. Top left: time evolution of Cα RMSD for all 44 peptide chains over a 500ns MD simulation. The five chains with the highest average RMSD are labeled while all others are shown in light traces. Top right: structural visualization of the fibril with the same five highest RMSD chains colored to indicate their changes. Initial structure is transparent while final structure is solid. Bottom: summary of per-chain RMSD values. Bars show the last frame while black dots indicate the average RMSD over the trajectory. Colored bars correspond to the highlighted chains in the time evolution plot.

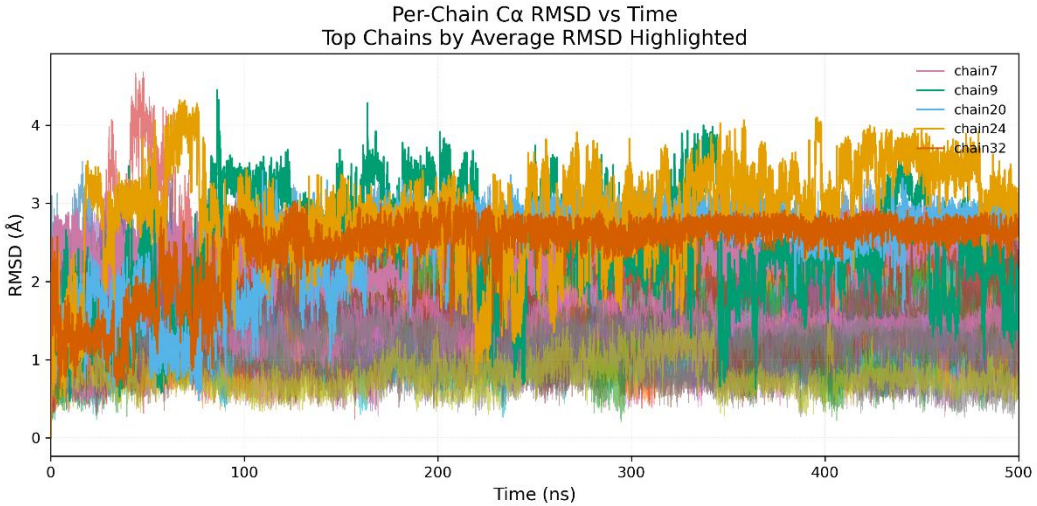

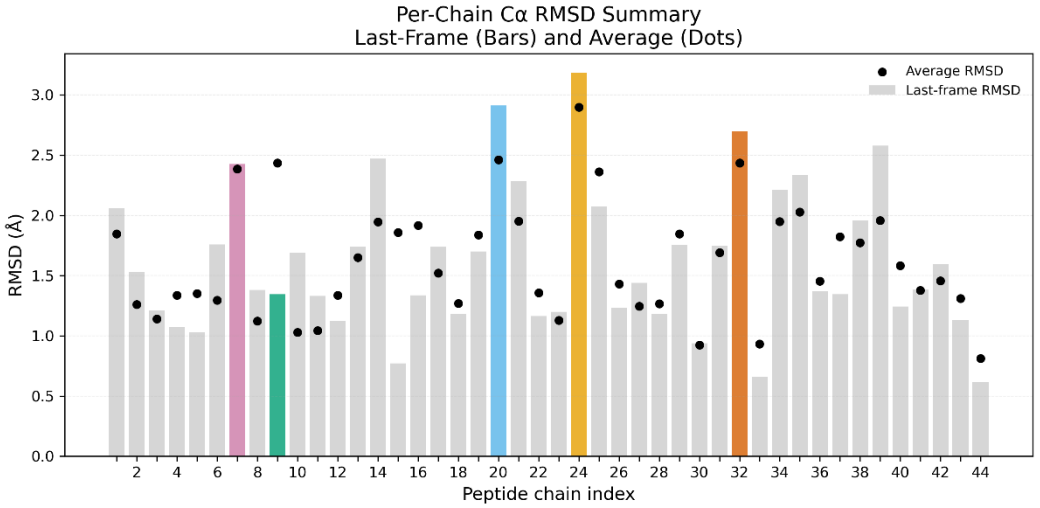

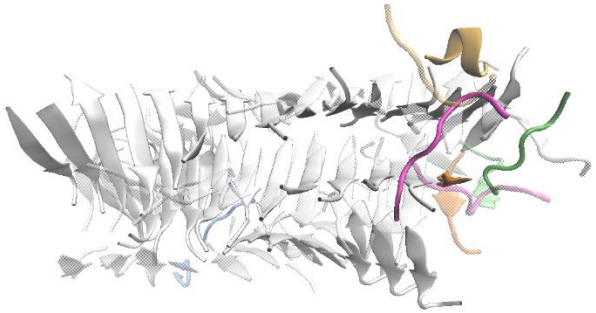

Figure S31 Per-chain structural stability analysis of P1-L38M fibril during MD Run 3. Top left: time evolution of Cα RMSD for all 44 peptide chains over a 500ns MD simulation. The five chains with the highest average RMSD are labeled while all others are shown in light traces. Top right: structural visualization of the fibril with the same five highest RMSD chains colored to indicate their changes. Initial structure is transparent while final structure is solid. Bottom: summary of per-chain RMSD values. Bars show the last frame while black dots indicate the average RMSD over the trajectory. Colored bars correspond to the highlighted chains in the time evolution plot.

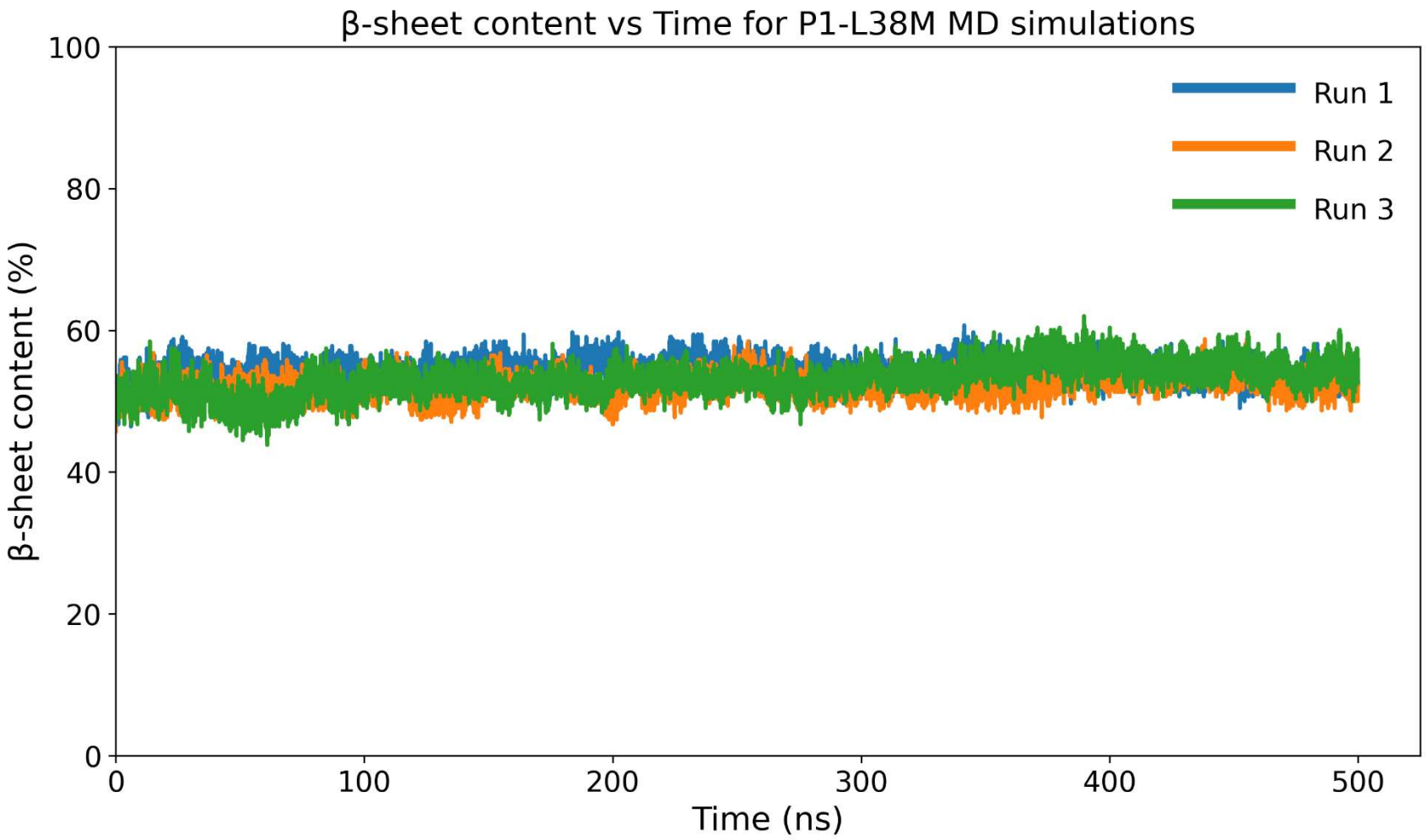

Figure S32 Time evolution of β-sheet content across three independent MD simulations of atomistic-resolution P1-L38M fibril reconstructed from DMD/PRIME20 simulation.

Supplementary Method:

Statistical Power Analysis and Sample Size Estimation:

To evaluate whether the number of independent simulations for each peptide variant was sufficient to detect statistically significant differences in β-hairpin content among P3Next variants, we performed a two-sample statistical power analysis (Cohen 2013) based on the observed means and standard deviations from the existing simulations. The two-tailed test for inequal sample sizes method were applied in our calculation. For each variant, the standardized effect size index (Cohen's d) for a nondirectional (two-tailed) case was calculated relative to P3Next-WT as:

$$d = |m_{variant} - m_{WT}| / s_p$$

where

- m is defined as the population mean of original measurement. In our research, m denotes the mean β-hairpin percentage of seven runs for each peptide sequence.
- s_p is the pooled standard deviation (Moore et al. 2009),

$$s_p = \mathrm{sqrt}(((n_1 - 1)s_1^2 + (n_2 - 1)s_2^2) / (n_1 + n_2 - 2))$$

with s_1, s_2 and n_1, n_2 being the standard deviations and the number of simulations runs for each variant, respectively.

The required number of simulations per variant (n) to detect the observed effect was estimated using the standard normal approximation to the two-sample t-test. We chose settings that limit the chance of falsely identifying a difference to 5% ($\alpha = 0.05$) and the chance of missing a real difference to 20% ($\beta = 0.2$), which are commonly used in scientific studies (Cohen 2013).

$$n = 2 \times ((z_{(\alpha/2)} + z_{(1-\beta)}) / d)^2$$

where $z_{(\alpha/2)}$ and $z_{(1-\beta)}$ are the critical z-values from the standard normal distribution corresponding to the chosen significance level (α) and desired power (1-β)(Cohen 2013). For $\alpha = 0.05$ and $\beta=0.2$, the corresponding values of $z_{(\alpha/2)}$ and $z_{(1-\beta)}$ are 1.96 and 0.84, respectively.

$$n = 2 \times (2.80 / d)^2$$

This formula quantifies the minimum number of independent trajectories required for each variant and WT. Larger effect sizes (greater d) require fewer trajectories, whereas smaller effects demand more extensive sampling. The results are shown in **Table S2**.

Table S3. Statistical power analysis of β-hairpin content differences between P3Next variants and P3Next-WT.

Mutated variant	Total runs (variant, WT)	Average % of β-hairpins (variant, WT)	Δ	Pooled SD s_p	Cohen's d	Number of runs needed
L38M	7, 7	16, 23	7	3.73	**1.85**	**5**
L38A	5, 7	46, 23	23	10.85	**2.11**	**4**
V40A	6, 7	36, 23	13	10.54	**1.30**	**9**
Y39A	7, 7	30, 23	7	5.93	**1.16**	**12**
S42A	7, 7	23, 23	0	5.77	**0.10**	**1671**

Supplementary Movies:

We also attached all Supplementary Movies for examples of aggregation process through the entire DMD/PRIME20 simulations. DMD/PRIME20 uses periodic boundary conditions. Therefore, the peptides would enter the opposite boundary when there was a boundary causing the peptides or fibrils to segment although they were still connected.

Supplementary Movie 1: An example of P1-WT Run 1 simulation

https://github.com/CarolHall-NCSU-CBE/Alpha-Synuclein-Nterminal-Fragments-Simulations-VN/blob/main/movies/Supplementary%20Movie%201%20P1-WT-Run1%20.mpg

Supplementary Movie 2: An example of P2 Run 1 simulation that formed U-shape β-sheet

https://github.com/CarolHall-NCSU-CBE/Alpha-Synuclein-Nterminal-Fragments-Simulations-VN/blob/main/movies/Supplementary%20Movie%202%20P2-Run1-Ushape.mpg

Supplementary Movie 3: An example of P2 Run 3 simulation that formed S-shape β-sheet

https://github.com/CarolHall-NCSU-CBE/Alpha-Synuclein-Nterminal-Fragments-Simulations-VN/blob/main/movies/Supplementary%20Movie%203%20P2-Run3-Sshape.mpg

Supplementary Movie 4: An example of P3-WT Run 3 simulation

https://github.com/CarolHall-NCSU-CBE/Alpha-Synuclein-Nterminal-Fragments-Simulations-VN/blob/main/movies/Supplementary%20Movie%204%20P3-WT-Run3.mpg

Supplementary Movie 5: An example of P3Next-WT Run 4 simulation

https://github.com/CarolHall-NCSU-CBE/Alpha-Synuclein-Nterminal-Fragments-Simulations-VN/blob/main/movies/Supplementary%20Movie%205%20P3Next-WT-Run4.mpg

REFERENCES

Cohen, Jacob. 2013. *Statistical Power Analysis for the Behavioral Sciences*. 0 ed. Routledge. https://doi.org/10.4324/9780203771587.

Moore, David S., George P. McCabe, and Bruce A. Craig. 2009. *Introduction to the Practice of Statistics*. 6th ed. W.H. Freeman.

Rodriguez, Jose A., Magdalena I. Ivanova, Michael R. Sawaya, et al. 2015. "Structure of the Toxic Core of α-Synuclein from Invisible Crystals." *Nature* 525 (7570): 486–90. https://doi.org/10.1038/nature15368.